Biological Chemistry ‘Just Accepted’ Papers

Biological Chemistry ‘Just Accepted’ Papers are papers published online, in advance of appearing in the print journal. They have been peer-reviewed, accepted and are online published in manuscript form, but have not been copy edited, typeset, or proofread. Copy editing may lead to small differences between the Just Accepted version and the final version. There may also be differences in the quality of the graphics. When papers do appear in print, they will be removed from this feature and grouped with other papers in an issue.

Biol Chem ‘Just Accepted’ Papers are citable; the online publication date is indicated on the Table of Contents page, and the article’s Digital Object Identifier (DOI), a unique identifier for intellectual property in the digital environment (e.g., 10.1515/hsz-2011-xxxx), is shown at the top margin of the title page. Once an article is published as **Biol Chem ‘Just Accepted’ Paper** (and before it is published in its final form), it should be cited in other articles by indicating author list, title and DOI.

After a paper is published in **Biol Chem ‘Just Accepted’ Paper** form, it proceeds through the normal production process, which includes copy editing, typesetting and proofreading. The edited paper is then published in its final form in a regular print and online issue of **Biol Chem.** At this time, the **Biol Chem ‘Just Accepted’ Paper** version is replaced on the journal Web site by the final version of the paper with the same DOI as the **Biol Chem ‘Just Accepted’ Paper version.**

Disclaimer

Biol Chem ‘Just Accepted’ Papers have undergone the complete peer-review process. However, none of the additional editorial preparation, which includes copy editing, typesetting and proofreading, has been performed. Therefore, there may be errors in articles published as **Biol Chem ‘Just Accepted’ Papers** that will be corrected in the final print and online version of the Journal. Any use of these articles is subject to the explicit understanding that the papers have not yet gone through the full quality control process prior to advanced publication.

Biological Chemistry **'Just Accepted' paper**
ISSN (online) 1437-4315
DOI: 10.1515/hsz-2019-0109

Research Article

Indigoid dyes by group E monooxygenases: mechanism and biocatalysis

Thomas Heine[1], Carolin Großmann[1], Sarah Hofmann[1] and Dirk Tischler[1,2,]*

[1]Institute of Biosciences, Environmental Microbiology, TU Bergakademie Freiberg, Leipziger Str. 29, D-09599 Freiberg, Germany

[2]Microbial Biotechnology, Ruhr University Bochum, Universitätsstr. 150, D-44780 Bochum, Germany

*Corresponding author

e-mail: dirk.tischler@rub.de

Abstract

Since ancient times, people are attracted by dyes and they were a symbol of power. Some of the oldest dyes are indigo and its derivative Tyrian purple, which were extracted from plants and snails, respectively. These “indigoid dyes” were and are still used for coloration of textiles and as a food additive. The traditional Chinese medicine also knows indigoid dyes as pharmacologically active compounds and several studies support their effect. Further, they are interesting for future technologies like organic electronics. In these cases, especially the indigo derivatives are of interest but unfortunately hardly accessible by chemical synthesis. In recent decades, more and more enzymes have been discovered that are able to produce these indigoid dyes and therefore gained attention from the scientific community. In this study, group E monooxygenases (styrene monooxygenase and indole monooxygenase) were used for the selective oxygenation of indole (derivatives). It was possible for the first time to show that the product of the enzymatic reaction is an epoxide. Further, we synthesized and extracted indigoid dyes and could show that there is only minor by-product formation (e.g. indirubin or isoindigo). Thus, group E monooxygenase can be an alternative biocatalyst for the biosynthesis of indigoid dyes.

Keywords: dye production; epoxidation; flavoprotein; indole monooxygenase; styrene monooxygenase.

Introduction

One of the oldest pigments used by humans is Tyrian purple. It was and is one of the most valuable dyes as a gram still costs about 3000 €. Tyrian purple, which is chemically 6,6`-dibromoindigo, is a derivative of the well-known denim colorant indigo. Substituted indigo derivatives are termed as indigoid dyes (Figure 1). In recent years, these indigoid dyes gained interest in several other application areas, as they represent interesting candidates for pharmaceutical, food and semiconductor industries (Ma *et al.*, 2018b). In particular, indigoid dyes have been shown to function as antibiotic (Namgung *et al.*, 2019) and against several types of cancer as they have antineoplastic or antileukemic activity (Xiao *et al.*, 2002; Dua *et al.*, 2014). Furthermore, they have hemostatic, antipyretic, anti-inflammatory, and sedative properties (Dua *et al.*, 2014). Thus, they are among others of interest for the treatment of allergies, Alzheimer's disease and delayed hypersensitivity (Kapadia *et al.*, 1998; Wu *et al.*, 2005; Hössel 1999; Hoessel *et al.*, 1999; Guengerich *et al.*, 2004a,b; Eisenbrand *et al.*, 2004; Leclerc *et al.*, 2001; Kunikata *et al.*, 2000; Lin *et al.*, 2012; Dua *et al.*, 2014; McClay *et al.*, 2005; Farias-Silva *et al.*, 2007; Pathak and Madamwar 2010; Xiao *et al.*, 2002). A recent study showed that encapsulation of indigoid dyes into inorganic hosts can be useful for the production of hybrid pigments and photo-functional materials (Petermayer and Dube, 2018). Moreover, they can be used in dye-containing polymers, photoswitches, on memory chips and in high-performance organic semiconductors (Petermayer and Dube, 2018; Fleischmann *et al.*, 2015; Harrer, 2012; Uehara *et al.*, 1987; Irimia-Vladu *et al.*, 2012; He *et al.*, 2014; Głowacki *et al.*, 2012). In the latter case, especially the high-cost derivative Tyrian purple is of interest. Thus, it is of importance to produce indigoid molecules selectively in order to have pure compounds for the subsequent applications.

While indigo itself is already produced at industrial scale (about 50 000 tonnes per year), the indigo derivatives are hardly accessible by chemical means. Therefore, bacterial sources for the production of indigoid dyes have been exploited for several years and the biosynthesis routes of indigoid dyes can be seen as one alternative of aerobic indole detoxification. The other alternative is the degradation of indole to use it as a source for carbon and energy (Arora *et al.*, 2015; Ma *et al.*, 2018b).

Indole and its derivatives are widely distributed in the environment as they occur naturally in alkaloids, phytohormones, plant flower oils, pigments, fossil organic matter, signaling molecule and product of the tryptophan metabolism but also anthropogenically as product of

pharmaceutical industries (Lee *et al.*, 2015; Arora *et al.*, 2015; Sharma *et al.*, 2010; Ma *et al.*, 2018b). Due to that extensive exposure, a variety of microorganisms was found to be able to degrade and transform indole and in the course of that, many enzymes (monooxygenases and dioxygenases) were identified that enable the formation of indigoid dyes (reviewed in Heine *et al.*, 2018a; Ma *et al.*, 2018b). These often initiate the degradation of indole by mono- or dioxygenation at the double bond of the pyrrole moiety or at the benzene moiety (Heine *et al.*, 2018a). Intermediates of these reactions that were often detected are indoxyl, dihydroxyindole, indole-2,3-dihydroindole and oxindole leading to isatin and/or anthranilate as central intermediates (Fukuoka *et al.*, 2015; Yuan, 2011; Sadauskas *et al.*, 2017; Fujioka and Wada, 1968; Ma *et al.*, 2018b).

Despite the fact that many oxidoreductases were identified that are able to oxidize indole, for most of them it seems to be not the natural substrate (Ma *et al.*, 2018b). However, recently identified monooxygenases (IndA, IifC) were found in *Acinetobacter, Burkholderia* and *Cupriavidus* strains located in a gene cluster that enables indole degradation in these bacteria (Sadauskas *et al.*, 2017; Lin *et al.*, 2015; Qu *et al.*, 2017; Zhang *et al.*, 2018; Ma *et al.*, 2018a). This and an associated anthranilate degradation cluster has already been identified by Tischler *et al.*, in 2012 and was proposed to be involved in aromatic compound degradation (Tischler *et al.*, 2012). The initiating monooxygenases were originally assigned as styrene monooxygenase (group E monooxygenase, GEM) due to sequence homology. GEMs are flavin adenine dinucleotide (FAD) dependent enzymes, which require for a nicotinamide adenine dinucleotide (NADH) dependent FAD reductase as the second component for the supply of reduced cosubstrate (Montersino *et al.*, 2011). However, in accordance with the recent findings, GEMs have been divided into two subgroups: styrene monooxygenase (SMO) and indole monooxygenase (IMO) (Heine *et al.*, 2018b). Finally, the monooxygenases IndA and IifC can now be assigned to the latter group of IMOs where indole is supposed to be the natural substrate.

However, it is to date not solved, which product is actually formed by IMOs: indole oxide or directly indole-2,3-dihydrodiol (Boyd *et al.*, 1997; O'Connor *et al.*, 1997; Sadauskas *et al.*, 2017). In this study, we established a method published by Dupard-Julien *et al.*, 2007 to clarify this issue. Therefore, we selected four GEMs that were initially characterized by Heine *et al.* (2018a): *Ab*IndA is known to be part of a gene cluster that allows for indole biodegradation. *Vp*IndA1 is located in a gene cluster also containing the respective indole degradation genes and in addition a fusion protein of the IMO. It was proven a promising

sulfoxidase (Tischler *et al.*, 2018). *Ro*IndA1 is part of a similar gene cluster while one gene that is supposed to be required for indole degradation is disrupted (Tischler *et al.*, 2012). *Ro*IndA1 is one of the best-studied IMOs (Tischler *et al.*, 2010; Riedel *et al.*, 2015; Paul *et al.*, 2015). Additionally, the SMO *Gp*StyA was included as it showed one of the highest activities of all GEMs in preliminary tests.

These GEMs were used for the production of indigoid dyes, which were identified by Vis-spectral and MS analysis.

Results

Biotransformation of Indole Derivatives to Indigoid Dyes

The four monooxygenases have been successfully produced recombinantly in *Escherichia coli* as described previously (Tischler *et al.*, 2009, 2018; Riedel *et al.*, 2015). During gene expression, the cells turned dark blue, which is an indication of indigo formation. This happens due to tryptophanase (TnaA) activity of host cells leading to significant amounts of indole from tryptophan (Li and Young, 2013), which is subsequently oxygenated by the present recombinant monooxygenases. It indicated a successful enzyme production. The proteins were obtained at high purity (yield of 3 to 38 mg enzyme l^{-1}, depending on type and culture medium) and were subsequently assayed for styrene epoxidation activity. They showed activities as follows; *Gp*StyA (570 ± 90 mU mg^{-1}) > *Ab*IndA (139 ± 16 mU mg^{-1}) > *Ro*IndA1 (121 ± 22 mU mg^{-1}) ≥ *Vp*IndA1 (121 ± 9 mU mg^{-1}). In all cases the (*S*)-enantiomer was formed at high selectivity (> 94% ee) (Heine *et al.*, 2018a). These rates and enantioselectivity are in a comparable range to a number of previously investigated styrene epoxidizing enzymes (range 26 to 2100 mU mg^{-1}) (Otto *et al.*, 2004; van Hellemond *et al.*, 2007; Tischler *et al.*, 2010, 2018; Toda *et al.*, 2012; Tan *et al.*, 2019; Gursky *et al.*, 2010; Riedel *et al.*, 2015).

As group E monooxygenases are two-component flavoprotein monooxygenases, they rely on a support of reduced FAD in order to perform catalysis. To circumvent additional enzymes and cofactor limitation, the assays were performed with 1-Benzyl-1,4-dihydronicotinamide (BNAH) as direct FAD reductant (Paul *et al.*, 2015). For each enzyme, a concentration-dependent performance was determined (Figure 2). It turned out that all four enzymes behave

similarly with respect to BNAH supply with an optimal concentration between 8 and 12 mM. For the other experiments, the BNAH concentration was set to 10 mM.

Having those active monooxygenases and proper support of reduced FAD for catalysis, an assay for indole oxygenation was set up as described in the materials and methods section. The following substrates, indole, 6-fluoroindole, 6-chloroindole and 6-bromoindole were applied and the formation of respective indigoid dyes was followed spectrophotometrically (Figure 3). Herein it has to be mentioned, that the monooxygenases reach between 6 and 80% activity with indole compared to styrene: *Vp*IndA1 (80%) > *Ab*IndA (60%) > *Ro*IndA1 (17%) > *Gp*StyA (6%). Except for *Ro*IndA1, unsubstituted indole is the best substrate for all monooxygenases (Figure 3). The halogenated derivatives reach an activity of only about 20 to 60% if compared to indole. Interestingly, while 6-fluoroindole is not a good substrate for *Ro*IndA1, the chlorinated and brominated analogs work as good as the unsubstituted indole.

The extinction coefficients that either had been obtained from literature or that were determined from the upscaling experiments (Figure 4 and 5) were employed to calculate kinetic parameters. However, as discussed above this might not provide actual access on the monooxygenase functionality as several catalytic steps occur in the reaction course of indole to indigo. This is true for the derivatives as well. Despite this remark, there was still some variance determined from the kinetic experiments, which might be due to a different substrate acceptance of enzymes or due to a different dimerization velocity of generated indoxyl derivatives, respectively.

In order to produce more dye from the three different halogenated substrates upscaling experiments were performed with *Vp*IndA1 and *Gp*StyA. We obtained an amount of 2.3 to 5.5 mg halogenated indigoid dyes as well as 1.3 to 5.4 mg dimethoxy-substituted indigoid dyes (Table 1). This indicates that the conversion is better if the halogen substituent is bigger and/or has a lower electronegativity and that substitution is beneficial at the 5-position compared to 6- and 7-substituted indoles. However, this might be different depending on the respective enzyme.

An FT-ICR-MS analysis was done to identify the generated dyes. It should be mentioned, that this method does not discriminate between the indigo and the structural isomers indirubin and isoindigo. However, indirubin is much more stable as indigo in organic solvents and should get visible after a certain time (Meyer, 2002). We investigated that for several

biotechnologically produced dyes but did neither detect a corresponding change in color nor an absorbance shift to lower wavelengths in DMSO (Perpète *et al.*, 2006). Thereof, we hypothesize that mainly indigo (derivatives) are formed by GEMs, what remains to be proven by additional analysis.

However, Table S2 summarizes the results of the mass-spectrometry assignment. The observed mass-to-charge ratio fits the calculated ratios for the expected products.

Tracing epoxide formation by GEMs

As mentioned above, the intermediate that is formed by the monooxygenase IndA is yet unknown due to instability. Although several hypotheses about this intermediate were published, we presumed an epoxide to be formed by IMOs, as GEMs are generally known to act as epoxidases on double bonds. To clarify this, we attempted to trap the epoxide intermediate by derivatization with *N,N*-diethyldithiocarbamate (DTC) by an adapted method of Dupard-Julien *et al.*, 2007 (see materials and methods section). The expected derivatization mechanism is displayed in Scheme 1.

In advance to an enzymatic conversion, we performed control experiments to exclude unspecific reactions with other possible products or interference with components of the reaction mixture (see supplemental material section 1 and 2). Only the analogical indene oxide was derivatized by DTC treatment demonstrating the general functionality of the method (Figure 6A). For the enzymatic assays, we initially conducted the derivatization at 70°C after the ending of the reaction. This attempt was successful and an additional peak was observed eluting about 5 min later than the substrate indole (Figure 6B). The peak area increased slightly after a biotransformation time up to 10 min. However, parts of the product continued to react as the formation of indigo was still observed. The derivatization was shown to be temperature dependent (Dupard-Julien *et al.*, 2007). Nevertheless, to lower the derivatization temperature to 30°C was also appropriate and allowed to meet the enzymatic reaction conditions (supplementary material, section 1). Therewith, it was feasible to add DTC directly to the enzymatic reaction and to trap the epoxide immediately after formation by the IMO.

The identified product peak was collected after RP-HPLC and subjected to FT-ICR-MS analysis. The observed mass-to-charge ratio matches the expected ratio for the proposed hydroxyindole derivative (Table S1, Scheme 1).

Discussion

In this study, we selected four GEMs that have been characterized previously (*Ro*IndA1, accession number: ACR43973; *Vp*IndA1, ADU39063; *Ab*IndA, CAG69430 and *Gp*StyA, GAB22407). All of them perform selectively oxygenations on styrene and indole (-derivatives). Styrene and indole degradation are also the two physiological roles described for GEMs so far (Heine *et al.*, 2018b). However, analysis of the genomic neighborhood of GEMs indicated, that further functions in aromatic compound degradation are possible.

SMOs are often situated in a styrene degradation cluster allowing for conversion of styrene into phenylacetaldehyde as central intermediate (Tischler *et al.*, 2012; Heine *et al.*, 2018c). For several other SMOs, the physiological role is unclear, e.g. for *Gp*StyA which has no genes in the surrounding that are related to aromatic compound degradation. In contrast, a highly similar SMO from *Prauserella rugosa* NRRL B-2295 (WP_030532027) is located close to a phenol hydroxylase and subsequent enzymes for the attack at the aromatic ring. Thereof, it might be possible that styrene is degraded in this strain by oxidation at the vinyl side chain as well as at the aromatic ring system.

The second group of GEMs, IMOs, was recently classified as an independent subgroup and these monooxygenases are proposed to be involved in indole degradation (Sadauskas *et al.*, 2017; Heine *et al.*, 2018b) (Figure 7A). The core gene clusters that can be deduced from the genomic analysis, in which IMO-like enzymes were found, are illustrated in Figure 7B. The representative cluster (cluster 1) was identified in *Acinetobacter* and *Cupriavidus*. It contains a monooxygenase (IndA, IifC), an associated reductase (IndB, IifD), a short chain dehydrogenase (SDR) family protein (IndC, IifB) and a dienelactone hydrolase (DLH) family protein (IndD, IifA). The resulting enzyme cascade was described to constitute the upper indole degradation pathway to anthranilate as central intermediate (Gröning *et al.*, 2014; Sadauskas *et al.*, 2017; Zhang *et al.*, 2018; Lin *et al.*, 2015; Qu *et al.*, 2017) (Figure 7A). IndA catalyzes the oxygenation of indole to an unstable intermediate (*vide infra*) that can rapidly decompose to indoxyl, which dimerizes to indigo under aerobic conditions (O'Connor *et al.*, 1997; Sadauskas *et al.*, 2017). However, the indigo formation is prevented whenever IndC is present. Then, IndC immediately takes the unstable intermediate, and forms 3-hydoxyindolin-2-one, which is further converted by IndD to anthranilic acid (Sadauskas *et al.*, 2017). Genes for the lower degradation pathway from anthranilate to intermediates of

the tricarboxylic acid cycle were often found for representatives of cluster 1 in proximity or elsewhere on the genome (Table 2) (Zhang *et al.*, 2018).

Interestingly, we did not find anthranilate degradation genes in strains that harbor clusters 2 to 10 (Figure 7B). Indeed, genes related to the degradation of indolepyruvate and xanthine are adjacent (Table 2). Further, only cluster 1, 2 and 6 contain a complete set of genes to fulfill the described degradation route. The IMOs of *Variovorax paradoxus* EPS belong to the latter one. Herein, two IMOs are encoded whereby one is a fusion protein between the monooxygenase and a reductase part (IndA2B) (Tischler *et al.*, 2018). This special characteristic is known since 2009 when it was discovered and described for the first time for *Rhodococcus opacus* 1CP (Figure 7B, Cluster 7) (Tischler *et al.*, 2009). Both clusters (6 and 7) contain an SDR-like and a DLH-like protein, although the DLH is disrupted in strain 1CP. The fusion protein is supposed to act mainly as reductase component and the associated IndA1 enzymes also possess a much higher specific oxygenation activity (Tischler *et al.*, 2018; Tischler *et al.*, 2010). Just recently, a novel IMO has been identified in *Burkholderia* sp. IDO3, which is able to degrade indole (Cluster 10). It forms a separate branch from other IMOs as well as SMOs (Ma *et al.*, 2015, 2018a). Interestingly, only strains where the IMO is arranged in clusters like 1 and 10 have been proven capable to use indole as a source of carbon and energy (Table 2).

The fourth enzyme of this study is an SMO originating from *Gordonia polyisoprenivorans* NBRC 16320 (*Gp*StyA). Although classified as SMO, it is not part of a styrene degradation cluster and the physiological role is so far unclear. However, it has been shown to provide one of the highest epoxidation rates of GEMs and therefore was included in this study (unpublished).

Indole is widespread in the environment and many industrial products. The metabolic fate of indole has attracted greater interest in the last years, as many significant roles in prokaryotic but also eukaryotic organisms have been reported (Ma *et al.*, 2018b; Lee *et al.*, 2015; Kim and Park, 2015). In this study, we used IMOs for the biotransformation of indole to indigoid dyes. So far, only indole-2-monooxygenases (EC 1.14.13.137) are known to use indole as a physiological substrate for the biosynthesis of benzoxazinoids (Glawischnig *et al.*, 1999). Thus, IMOs are the first representatives reported to degrade indole as a physiological substrate. However, so far only strains that harbor IMO clusters like 1 and 10 have been reported to grow on indole (Table 2). Conscious that also the gene clusters for the degradation

of the intermediated anthranilate are missing in many cases, it has to be proven whether there are further routes for indole degradation or further roles of IMOs in that organisms. For example, the degradation of indolepyruvate or xanthine or the biosynthesis of other compounds.

All of the tested IMOs were able to produce indigoid dyes from indole precursors. We also tested styrene as a reference substrate. For all of the enzymes, the activity with indole is lower compared to styrene (Figure 3). For *Gp*StyA this corresponds to only about 6% of residual activity. This correlates with the fact that this enzyme is denoted as styrene epoxidizing monooxygenase and indole is not the physiological substrate.

It was possible to convert a variety of indole derivatives with GEMs that contain different substituents at various positions. In addition, the production of indigoid dyes with mixed substituents at both indole moieties is possible. This illustrates the broad applicability and product range that can be produced with GEMs. However, substituents at positions 2 and 3 of the indole heterocycle are problematic for the enzyme, what is reasonable, as this is the probable oxidation site.

Several hypotheses exist about the formed product. A possible route via an indole oxide and subsequent chemical or enzymatic hydrolysis to yield an indole-2,3-dihydrodiol followed by dehydration to yield indoxyl is discussed in literature (Boyd *et al.*, 1997; O'Connor *et al.*, 1997; Sadauskas *et al.*, 2017). Otherwise, the indole oxide can undergo an intramolecular rearrangement known as arene oxide-NIH shift reaction (Cerniglia *et al.*, 1984). Furthermore, styrene oxide isomerases catalyze such an intramolecular rearrangement and it was found that these enzymes are beneficial for indigo production employing styrene monooxygenases as initial catalysts (O'Connor *et al.*, 1997; Miyamoto *et al.*, 2007). However, the indigo formation does also happen in the absence of styrene oxide isomerase, thus two mechanisms might be possible in dependence of the environment. In case of dioxygenases, it was shown that indole gets di-oxygenated to the cis-indole-2,3-dihydrodiol which spontaneously dehydrates to indoxyl (Ensley *et al.*, 1983; Mermod *et al.*, 1986; Murdock *et al.*, 1993).

In this study, we were able to do a qualitative analysis of the formed product, an indole-2,3-oxide, for two different IMOs (*Ab*IndA and *Vp*IndA1). Therewith, we propose that GEMs convert indole to an unstable epoxide, which rapidly hydrolyzes to a diol (Scheme 2). This diol can rapidly decompose to indoxyl, which spontaneously dimerizes to indigo. However, as

soon as other enzymes grab the epoxide or the diol, further degradation to anthranilic acid is observed (Sadauskas *et al.*, 2017).

Conclusion

Indigoid dyes are interesting compounds for various applications. Enzyme cascades can be used to produce indigo derivatives in an eco-friendly manner (Namgung *et al.*, 2019). Together with novel strategies for the generation of water-soluble forms that make them easier to handle (Hsu *et al.*, 2018), these indigo derivatives are better accessible for industrial applications. GEMs are candidates for the production of these dyes and in particular, IMOs, as they use indole as a physiological substrate. In addition, we were able to prove for the first time that an IMO epoxidizes indole as an initial step of the indole degradation pathway.

Materials and methods

Chemicals, strains, gene expression, and protein purification

Styrene and indole(-derivatives) were purchased from Sigma (Steinheim, Germany), TCI (Eschborn, Germany), Carl Roth (Karlsruhe, Germany), ABCR (Karlsruhe, Germany), Fluorochem (Hadfield, Derbyshire, UK), Alfa Aaser (Karlsruhe, Germany).

E. coli DH5α was used for cloning purposes and *E. coli* Bl21 (DE3) pLysS was used for gene expression (Sambrook and Russell, 2001). *Ro*IndA1 was obtained by PCR amplification and *Vp*IndA1, *Ab*IndA and *Gp*StyA were ordered by gene synthesis as described previously (Tischler *et al.*, 2010, 2018; Riedel *et al.*, 2015). The codon usage of the latter constructs was adapted to that of *Acinetobacter baylyi* ADP1 (Riedel *et al.*, 2015). All monooxygenase genes were subcloned into a pET16bP vector system for expression.

Gene expression was done as described previously by induction with isopropyl-*β*-D-thiogalactopyranosid (Tischler *et al.*, 2010; Riedel *et al.*, 2015) or by using Terrific broth (TB) autoinduction medium (Studier, 2005). Successful protein synthesis was apparent by a blue color formation resulting due to the indigo production. The target enzymes were purified by immobilized metal ion chromatography as published earlier (Tischler *et al.*, 2010; Riedel *et al.*, 2015).

Enzyme assays and biotransformation of indole (-derivatives)

Initial activity determination was done by the standard group E monooxygenase assay with styrene as substrate (Tischler *et al.*, 2010; Riedel *et al.*, 2015). For all assays, NADH as an electron donor was replaced by the mimic 1-benzyl-1,4-dihydronicotinamide (BNAH) (Paul *et al.*, 2015). The ideal BNAH addition was determined by means of separate standard assays with varying BNAH concentrations between 3 and 14 mM.

Additionally, indole(-derivatives) were supplied as substrate by means of the standard monooxygenase assay but in a 96 well plate. Formation of respective indigoid dyes was monitored spectrophotometrically (SpectraMax M2e; SoftMax Pro; Molecular Devices, USA). Therefore, UV/Vis-spectra (330-730 nm) of each indigoid dye was monitored over 2 h at 10 min intervals. Maximum absorption of each product was plotted over time to determine the specific activity.

Tracing of the indole-epoxide formation

Formation of epoxides during GEM conversion of indole was done according to the protocol of Dupard-Julien *et al.* (2007). After the enzymatic reaction, the epoxide is derivatized with *N,N*-diethyldithiocarbamate (DTC; 30°C or 70°C for 20 min) and unreacted DTC is eliminated by acidification with H_3PO_4. In a second attempt, we added DTC directly to the assay to extract the epoxide immediately from the reaction mixture and prevent its potential decomposition. Indole, 1-indanol, isatin, indene, and 1-phenyl-1,2-ethanediol served as controls but should not be derivatized by the method. The enzymatic reaction was set up according to the standard monooxygenase assay as described in the previous section. Therefore, *Ab*IndA was applied as biocatalyst and indole was used as substrate. Due to the instability of indole-2,3-oxide, we used indene-1,2-oxide as a reference compound. The derivatives were applied to RP-HPLC analysis using a Eurospher C18 column (125 mm length × 4 mm i.d., 5 mm particle size, 100 Å pore size; Knauer, Berlin, Germany) with a 40 to 75% acetonitrile gradient over 10 min at a flow rate of 1 ml min^{-1} (25°C). Eluting substances were monitored with a UV/Vis-detector. The detected product peak containing the generated derivative was collected, concentrated and subjected to mass spectrometry.

Upscaling, indigo purification, and spectral analysis

Upscaling of dye production was done by means of 25 ml assays for halogenated and methoxy-substituted indoles. The assays contained the following components: glycerol (5% v/v), Tris-HCl buffer (20 mM pH 7.5), dithiothreitol (1 mM), catalase (20.8 U ml^{-1}), FAD (50 µM), BNAH (10 mM) and the respective substrate (2 mM). The mixed components were tempered to 30°C and the reaction was started by addition of enzyme (2.8 mg). After 1 h reaction at 30°C (120 rpm), the produced indigoid dye was pelleted by centrifugation (11 000 *g*). The supernatant was removed; the pellet was washed twice with 2 ml dH_2O and dried at 60°C for 22 h. The product was weighed and partially dissolved in DMSO. Non-dissolved dye was removed from the solution by centrifugation and extinction was measured at the respective absorption maximum. DMSO was removed at 60°C under vacuum and the resulting pellet was weighed. The amount of indigoid dye that was dissolved in DMSO was calculated by the mass difference before and after dissolution experiments. The extinction coefficient in DMSO was calculated for each indigoid dye according to Lambert-Beers law ($E = \varepsilon \cdot c \cdot d$). The generated indigoid dyes were subjected to mass spectrometry.

Mass spectrometry

Fourier-transform ion cyclotron resonance mass spectrometry (FT-ICR-MS) experiments were conducted on a 15 T solariX FT-ICR-MS from Bruker Daltonics, equipped with an LDI source and operated in negative ion mode, with a scan range from 46.06 to 1000.00 Da. Resulting data sets had a size of 8 M and 16 scans were accumulated for each analysis. The sample was prepared directly by applying 1.5 µl of the undiluted sample solution per spot on a stainless steel target. For LDI analyses a Smartbeam II laser (frequency tripled Nd:Y laser, $\lambda = 355$ nm, 3 ns pulse duration, 500 µJ pulse energy) in the integrated LDI source was used. Furthermore, a medium focus, 20 or 250 laser shots per ICR fill and a fixed laser power of 40% or 70% were used for the sample analysis of indigoid dyes and the DTC-derivative, respectively.

Peak picking, calibration, and molecular formula assignment were accomplished using Bruker Daltonics software DataAnalysis 5.0 (SR1).

Acknowledgments

This research was funded by the Saxon Government (SAB) grant number 100263733 and the DECHEMA (Max-Buchner Fellowship to D.T.) grant number MBFSt 3339. We thank Jan Zuber from the Institute for Analytical Chemistry and Lucas Siegel (TU Bergakademie Freiberg) for support in the implementation of the analytics.

References

Arora, P.K., Sharma, A., and Bae, H. (2015) Microbial degradation of indole and its derivatives. J. Chem. *2015*, 1–13.

Boyd, C., Larkin, M.J., Reid, K.A., Sharma, N.D., and Wilson, K. (1997) Metabolism of naphthalene, 1-naphthol, indene, and indole by *Rhodococcus* sp. strain NCIMB 12038. Appl. Environ. Microbiol. *63*, 151–155.

Cerniglia, C.E., Freeman, J.P., and Evans, F.E. (1984) Evidence for an arene oxide-NIH shift pathway in the transformation of naphthalene to 1-naphthol by *Bacillus cereus*. Arch. Microbiol. *138*, 283–286.

Dua, A., Chauhan, K., and Pathak, H. (2014) Biotransformation of indigo pigment by indigenously isolated *Pseudomonas* sp. HAV-1 and assessment of its antioxidant property. Biotechnol. Res. Int. *2014*, 109249.

Dupard-Julien, C.L., Kandlakunta, B., and Uppu, R.M. (2007) Determination of epoxides by high-performance liquid chromatography following derivatization with *N,N*-diethyldithiocarbamate. Anal. Bioanal. Chem. *387*, 1027–1032.

Eisenbrand, G., Hippe, F., Jakobs, S., and Muehlbeyer, S. (2004) Molecular mechanisms of indirubin and its derivatives: novel anticancer molecules with their origin in traditional Chinese phytomedicine. J. Cancer Res. Clin. Oncol. *130*, 627–635.

Ensley, B.D., Ratzkin, B.J., Osslund, T.D., Simon, M.J., Wackett, L.P., and Gibson, D.T. (1983) Expression of naphthalene oxidation genes in *Escherichia coli* results in the biosynthesis of indigo. Science *222*, 167–169.

Farias-Silva, E., Cola, M., Calvo, T.R., Barbastefano, V., Ferreira, A.L., Paula Michelatto, D. de*, et al.,* (2007) Antioxidant activity of indigo and its preventive effect against ethanol-induced DNA damage in rat gastric mucosa. Planta Med. *73*, 1241–1246.

Fleischmann, C., Lievenbrück, M., and Ritter, H. (2015) Polymers and dyes. developments and applications. Polymers *7*, 717–746.

Fujioka, M., and Wada, H. (1968) The bacterial oxidation of indole. Biochim. Biophys. Acta, Gen. Subj. *158*, 70–78.

Fukuoka, K., Tanaka, K., Ozeki, Y., and Kanaly, R.A. (2015) Biotransformation of indole by *Cupriavidus* sp. strain KK10 proceeds through N-heterocyclic- and carbocyclic-aromatic ring cleavage and production of indigoids. Int. Biodeterior. Biodegradation *97*, 13–24.

Glawischnig, E., Grün, S., Frey, M., and Gierl, A. (1999) Cytochrome P450 monooxygenases of DIBOA biosynthesis. Specificity and conservation among grasses. Phytochemistry *50*, 925–930.

Głowacki, E.D., Voss, G., Leonat, L., Irimia-Vladu, M., Bauer, S., and Sariciftci, N.S. (2012) Indigo and tyrian purple – from ancient natural dyes to modern organic semiconductors. Isr. J. Chem. *52*, 540–551.

Gröning, J.A.D., Kaschabek, S.R., Schlömann, M., and Tischler, D. (2014) A mechanistic study on SMOB-ADP1: an NADH:flavin oxidoreductase of the two-component styrene monooxygenase of *Acinetobacter baylyi* ADP1. Arch. Microbiol. *196*, 829–845.

Guengerich, F.P., Martin, M.V., McCormick, W.A., Nguyen, L.P., Glover, E., and Bradfield, C.A. (2004a) Aryl hydrocarbon receptor response to indigoids in vitro and in vivo. Arch. Biochem. Biophys. *423*, 309–316.

Guengerich, F.P., Sorrells, J.L., Schmitt, S., Krauser, J.A., Aryal, P., and Meijer, L. (2004b) Generation of new protein kinase inhibitors utilizing cytochrome p450 mutant enzymes for indigoid synthesis. J. Med. Chem. *47*, 3236–3241.

Gursky, L.J., Nikodinovic-Runic, J., Feenstra, K.A., and O'Connor, K.E. (2010) *In vitro* evolution of styrene monooxygenase from *Pseudomonas putida* CA-3 for improved epoxide synthesis. Appl. Microbiol. Biotechnol. *85*, 995–1004.

Harrer, R. (2012) Indigo auf Speicherchips. Chemie in unserer Zeit *46*, 136.

He, B., Pun, A.B., Zherebetskyy, D., Liu, Y., Liu, F., Klivansky, L.M.*, et al.,* (2014) New form of an old natural dye: bay-annulated indigo (BAI) as an excellent electron accepting unit for high performance organic semiconductors. J. Am. Chem. Soc. *136*.

Heine, T., Großmann, C., Hofmann, S., and Tischler, D. (2018a) Enzymgesteuerte Indigoproduktion. Biospektrum *24*, 446–448.

Heine, T., van Berkel, W.J.H., Gassner, G., van Pée, K.-H., and Tischler, D. (2018b) Two-component fad-dependent monooxygenases. Current knowledge and biotechnological opportunities. Biology (Basel) *7*, 42.

Heine, T., Zimmerling, J., Ballmann, A., Kleeberg, S.B., Rückert, C., Busche, T.*, et al.,* (2018c) On the enigma of glutathione-dependent styrene degradation in *Gordonia rubripertincta* CWB2. Appl. Environ. Microbiol. *84*.

Hoessel, R., Leclerc, S., Endicott, J.A., Nobel, M.E., Lawrie, A., Tunnah, P.*, et al.,* (1999) Indirubin, the active constituent of a Chinese antileukaemia medicine, inhibits cyclin-dependent kinases. Nat. Cell Biol. *1*, 60–67, doi: 10.1038/9035.

Hössel, R. (1999) Synthese von Derivaten des Indirubins und Untersuchungen zur Mechanismusaufklärung ihrer antineoplastischen Wirkung.

Hsu, T.M., Welner, D.H., Russ, Z.N., Cervantes, B., Prathuri, R.L., Adams, P.D., and Dueber, J.E. (2018) Employing a biochemical protecting group for a sustainable indigo dyeing strategy. Nat. Chem. Biol. *14*, 256–261.

Irimia-Vladu, M., Głowacki, E.D., Troshin, P.A., Schwabegger, G., Leonat, L., Susarova, D.K.*, et al.,* (2012) Indigo--a natural pigment for high performance ambipolar organic field effect transistors and circuits. Adv. Mater. Weinheim *24*, 375–380.

Kapadia, G.J., Tokuda, H., Sridhar, R., Balasubramanian, V., Takayasu, J., Bu, P.*, et al.,* (1998) Cancer chemopreventive activity of synthetic colorants used in foods, pharmaceuticals and cosmetic preparations. Cancer Lett. *129*, 87–95.

Kim, J., and Park, W. (2015) Indole: a signaling molecule or a mere metabolic byproduct that alters bacterial physiology at a high concentration? J. Microbiol. *53*, 421–428.

Kunikata, T., Tatefuji, T., Aga, H., Iwaki, K., Ikeda, M., and Kurimoto, M. (2000) Indirubin inhibits inflammatory reactions in delayed-type hypersensitivity. Eur. J. Pharmacol. *410*, 93–100.

Leclerc, S., Garnier, M., Hoessel, R., Marko, D., Bibb, J.A., Snyder, G.L.*, et al.,* (2001) Indirubins inhibit glycogen synthase kinase-3 beta and CDK5/p25, two protein kinases involved in abnormal tau phosphorylation in Alzheimer's disease. A property common to most cyclin-dependent kinase inhibitors? J. Biol. Chem. *276*, 251–260.

Lee, J.-H., Wood, T.K., and Lee, J. (2015) Roles of indole as an interspecies and interkingdom signaling molecule. Trends Microbiol. *23*, 707–718.

Li, G., and Young, K.D. (2013) Indole production by the tryptophanase TnaA in Escherichia coli is determined by the amount of exogenous tryptophan. Microbiology (Reading) *159*, 402–410.

Lin, G.-H., Chen, H.-P., Huang, J.-H., Liu, T.-T., Lin, T.-K., Wang, S.-J., Tseng, C.-H., and Shu, H.-Y. (2012) Identification and characterization of an indigo-producing oxygenase involved in indole 3-acetic acid utilization by *Acinetobacter baumannii*. Antonie van Leeuwenhoek *101*, 881–890.

Lin, G.-H., Chen, H.-P., Shu, H.-Y., and Lee, S.-W. (2015) Detoxification of indole by an indole-induced flavoprotein oxygenase from *Acinetobacter baumannii*. PLoS ONE *10*, e0138798, doi: 10.1371/journal.pone.0138798.

Ma, Q., Liu, Z., Yang, B., Dai, C., and Qu, Y. (2018a) Characterization and functional gene analysis of a newly isolated indole-degrading bacterium *Burkholderia* sp. IDO3. J. Hazard. Mater. *367*, 144–151, doi: 10.1016/j.jhazmat.2018.12.068.

Ma, Q., Qu, Y., Zhang, X., Liu, Z., Li, H., Zhang, Z*., et al.,* (2015) Systematic investigation and microbial community profile of indole degradation processes in two aerobic activated sludge systems. Sci. Rep. *5*, 17674, doi: 10.1038/srep17674.

Ma, Q., Zhang, X., and Qu, Y. (2018b) Biodegradation and biotransformation of indole. Advances and perspectives. Front. Microbiol. *9*, 2625, doi: 10.3389/fmicb.2018.02625.

McClay, K., Boss, C., Keresztes, I., and Steffan, R.J. (2005) Mutations of toluene-4-monooxygenase that alter regiospecificity of indole oxidation and lead to production of novel indigoid pigments. Appl. Environ. Microbiol. *71*, 5476–5483, doi: 10.1128/AEM.71.9.5476-5483.2005.

Mermod, N., Harayama, S., and Timmis, K.N. (1986) New route to bacterial production of indigo. Nat. Biotechnol. *4*, 321–324, doi: 10.1038/nbt0486-321.

Meyer, A. (2002) Hydroxylation of indole by laboratory-evolved 2-hydroxybiphenyl 3-monooxygenase. J. Biol. Chem. *277*, 34161–34167, doi: 10.1074/jbc.M205621200.

Miyamoto, K., Okuro, K., and Ohta, H. (2007) Substrate specificity and reaction mechanism of recombinant styrene oxide isomerase from *Pseudomonas putida* S12. Tetrahedron Lett. *48*, 3255–3257, doi: 10.1016/j.tetlet.2007.03.016.

Montersino, S., Tischler, D., Gassner, G.T., and van Berkel, W.J.H. (2011) Catalytic and structural features of flavoprotein hydroxylases and epoxidases. Adv. Synth. Catal. *353*, 2301–2319, doi: 10.1002/adsc.201100384.

Murdock, D., Ensley, B.D., Serdar, C., and Thalen, M. (1993) Construction of metabolic operons catalyzing the de novo biosynthesis of indigo in *Escherichia coli*. Bio/technology (Nature Publishing Company) *11*, 381–386.

Namgung, S., Park, H.A., Kim, J., Lee, P.-G., Kim, B.-G., Yang, Y.-H., and Choi, K.-Y. (2019) Ecofriendly one-pot biosynthesis of indigo derivative dyes using CYP102G4 and PrnA halogenase. Dyes Pigm. *162*, 80–88, doi: 10.1016/j.dyepig.2018.10.009.

O'Connor, K.E., Dobson, A.D., and Hartmans, S. (1997) Indigo formation by microorganisms expressing styrene monooxygenase activity. Appl. Environ. Microbiol. *63*, 4287–4291.

Otto, K., Hofstetter, K., Röthlisberger, M., Witholt, B., and Schmid, A. (2004) Biochemical characterization of StyAB from *Pseudomonas* sp. strain VLB120 as a two-component

flavin-diffusible monooxygenase. J. Bacteriol. *186*, 5292–5302, doi: 10.1128/JB.186.16.5292-5302.2004.

Pathak, H., and Madamwar, D. (2010) Biosynthesis of indigo dye by newly isolated naphthalene-degrading strain *Pseudomonas* sp. HOB1 and its application in dyeing cotton fabric. Appl. Biochem. Biotechnol. *160*, 1616–1626, doi: 10.1007/s12010-009-8638-4.

Paul, C.E., Tischler, D., Riedel, A., Heine, T., Itoh, N., and Hollmann, F. (2015) Nonenzymatic regeneration of styrene monooxygenase for catalysis. ACS Catal. *5*, 2961–2965, doi: 10.1021/acscatal.5b00041.

Perpète, E.A., Preat, J., André, J.-M., and Jacquemin, D. (2006) An ab initio study of the absorption spectra of indirubin, isoindigo, and related derivatives. J. Phys. Chem. A *110*, 5629–5635, doi: 10.1021/jp060069e.

Petermayer, C., and Dube, H. (2018) Indigoid photoswitches. Visible light responsive molecular tools. Accounts of chemical research *51*, 1153–1163, doi: 10.1021/acs.accounts.7b00638.

Qu, Y., Ma, Q., Liu, Z., Wang, W., Tang, H., Zhou, J., and Xu, P. (2017) Unveiling the biotransformation mechanism of indole in a *Cupriavidus* sp. strain. Mol Microbiol, doi: 10.1111/mmi.13852.

Riedel, A., Heine, T., Westphal, A.H., Conrad, C., Rathsack, P., van Berkel, W.J.H., and Tischler, D. (2015) Catalytic and hydrodynamic properties of styrene monooxygenases from *Rhodococcus opacus* 1CP are modulated by cofactor binding. AMB Express *5*, 112, doi: 10.1186/s13568-015-0112-9.

Sadauskas, M., Vaitekūnas, J., Gasparavičiūtė, R., and Meškys, R. (2017) Indole biodegradation in *Acinetobacter* sp. strain O153. Genetic and biochemical characterization. Appl. Environ. Microbiol. *83, doi:* 10.1128/AEM.01453-17.

Sambrook J, Russell DW (eds.) (2001) *Molecular cloning. A laboratory manual.* Cold Spring Harbor, NY: Cold Spring Harbor Laboratory Press.

Sharma, V., Kumar, P., and Pathak, D. (2010) Biological importance of the indole nucleus in recent years. A comprehensive review. J. Heterocyclic Chem. *39*, NA-NA, doi: 10.1002/jhet.349.

Studier, F.W. (2005) Protein production by auto-induction in high density shaking cultures. Protein Expr. Purif. *41*, 207–234.

Tan, C., Zhang, X., Zhu, Z., Xu, M., Yang, T., Osire, T., Yang, S., and Rao, Z. (2019) Asp305Gly mutation improved the activity and stability of the styrene monooxygenase for efficient epoxide production in *Pseudomonas putida* KT2440. Microb. Cell. Fact. *18*, 12, doi: 10.1186/s12934-019-1065-5.

Tischler, D., Eulberg, D., Lakner, S., Kaschabek, S.R., van Berkel, W.J.H., and Schlömann, M. (2009) Identification of a novel self-sufficient styrene monooxygenase from *Rhodococcus opacus* 1CP. J. Bacteriol. *191*, 4996–5009, doi: 10.1128/JB.00307-09.

Tischler, D., Gröning, J.A.D., Kaschabek, S.R., and Schlömann, M. (2012) One-component styrene monooxygenases: an evolutionary view on a rare class of flavoproteins. Appl. Biochem. Biotechnol. *167*, 931–944, doi: 10.1007/s12010-012-9659-y.

Tischler, D., Kermer, R., Gröning, J.A.D., Kaschabek, S.R., van Berkel, W.J.H., and Schlömann, M. (2010) StyA1 and StyA2B from *Rhodococcus opacus* 1CP: a

Multifunctional styrene monooxygenase system. J. Bacteriol. *192*, 5220–5227, doi: 10.1128/JB.00723-10.

Tischler, D., Schwabe, R., Siegel, L., Joffroy, K., Kaschabek, S., Scholtissek, A., and Heine, T. (2018) VpStyA1/VpStyA2B of *Variovorax paradoxus* EPS. An aryl alkyl sulfoxidase rather than a styrene epoxidizing monooxygenase. Molecules (Basel, Switzerland) *23*, 809, doi: 10.3390/molecules23040809.

Toda, H., Imae, R., Komio, T., and Itoh, N. (2012) Expression and characterization of styrene monooxygenases of *Rhodococcus* sp. ST-5 and ST-10 for synthesizing enantiopure (*S*)-epoxides. Appl. Microbiol. Biotechnol. *96*, 407–418, doi: 10.1007/s00253-011-3849-3.

Uehara, K., Takagishi, K., and Tanaka, M. (1987) The Al/Indigo/Au photovoltaic cell. Solar Cells *22*, 295–301, doi: 10.1016/0379-6787(87)90059-7.

van Hellemond, E.W., Janssen, D.B., Fraaije, M.W., Janssen, D.B., and Fraaije, M.W. (2007) Discovery of a novel styrene monooxygenase originating from the metagenome. Appl. Environ. Microbiol. *73*, 5832–5839.

Wu, Z.-L., Aryal, P., Lozach, O., Meijer, L., and Guengerich, F.P. (2005) Biosynthesis of new indigoid inhibitors of protein kinases using recombinant cytochrome P450 2A6. Chem. Biodivers. *2*, 51–65, doi: 10.1002/cbdv.200490166.

Xiao, Z., Hao, Y., Liu, B., and Qian, L. (2002) Indirubin and meisoindigo in the treatment of chronic myelogenous leukemia in China. Leuk. Lymphoma *43*, 1763–1768, doi: 10.1080/1042819021000006295.

Yuan, L.-J. (2011) Biooxidation of indole and characteristics of the responsible enzymes. Afr. J. Biotechnol. *10, doi:* 10.5897/AJBX11.008.

Zhang, X., Jing, J., Zhang, L., Song, Z., Zhou, H., Wu, M., Qu, Y., and Liu, L. (2018) Biodegradation characteristics and genomic functional analysis of indole-degrading bacterial strain *Acinetobacter* sp. JW. J. Chem. Technol. Biotechnol., doi: 10.1002/jctb.5858.

Tables and figures

Table 1 Cell-free production of indigoid dyes by GEMs. The extinction coefficient of the produced dyes was determined in DMSO.

Product	Enzyme	Yield [mg]	Yield [%]	λ_{max} [nm]	Extinction coefficient$_{DMSO}$ [L mol^{-1} cm^{-1}]
Indigo	*Vp*IndA1	2.2	33.6	620	3660
6,6'-Difluoroindigo	*Gp*StyA	2.3	30.8	590	4271
6,6'-Dichloroindigo		3.4	41.1	605	3112
6,6'-Dibromoindigo		5.5	52.4	610	2506
5,5'-Dimethoxyindigo	*Vp*IndA1	5.4	67.0	665	1992
6,6'-Dimethoxyindigo		4.1	50.9	580	5709
7,7'-Dimethoxyindigo		1.3	16.1	620	13 036
6-Bromoindigo		4.3	50.4	610	1809

Table 2 Assignment of IMO-related gene clusters and adjacent genomic regions.

C	Strain	Adjacent Gene (Clusters)	Anthranilate degradation cluster on the genome
1	*Acinetobacter baylyi* ADP1*	Anthranilate degradation	Yes
	Acinetobacter sp. O153	Anthranilate degradation	Yes
	Acinetobacter sp. JW	Anthranilate degradation	Yes
	Acinetobacter baumannii ATCC19606	Anthranilate degradation	Yes
	Burkholderia sp. H160	-	Yes
	Cupriavidus sp. SHE	-	Yes
	Cupriavidus necator H16	-	Yes
	Halomonas halocynthiae DSM14573	Indolepyruvate degradation	Yes
	Marinobacterium stanieri S30	Anthranilate/catechol/phenol degradation	Yes
	Pseudomonas psychrotolerans NS337	Anthranilate/catechol/phenol degradation	Yes
2	*Delftia acidovorans* SPH-1	-	No
3	*Gemmobacter nectariphilus* DSM 15620	Indolepyruvate degradation	No
	Thermocrispum agreste DSM 44070	Xanthine degradation	No
	Sphingobacterium lactis DSM 22361	Indolepyruvate degradation	No
4	*Mesorhizobium sp.* F7	-	No
5	Gypsy moth gut metagenome	-	-
	Deep-sea sediment metagenome	Xanthine degradation	-
6	*Variovorax paradoxus* EPS*	-	No
7	*Rhodococcus opacus* 1CP*	-	No
8	*Nocardia farcinica* IFM 10152	-	No
	Paenarthrobacter aurescens TC1	Dehydrogenase/Cyclase	No
9	*Gordonia* sp. I37	-	No
	Streptomyces auratus AGR0001	Xanthine degradation	No
10	*Burkholderia* sp. IDO3	-	No

C – Cluster. Strains that are proven to degrade indole are underlined. *IMOs used in this study.

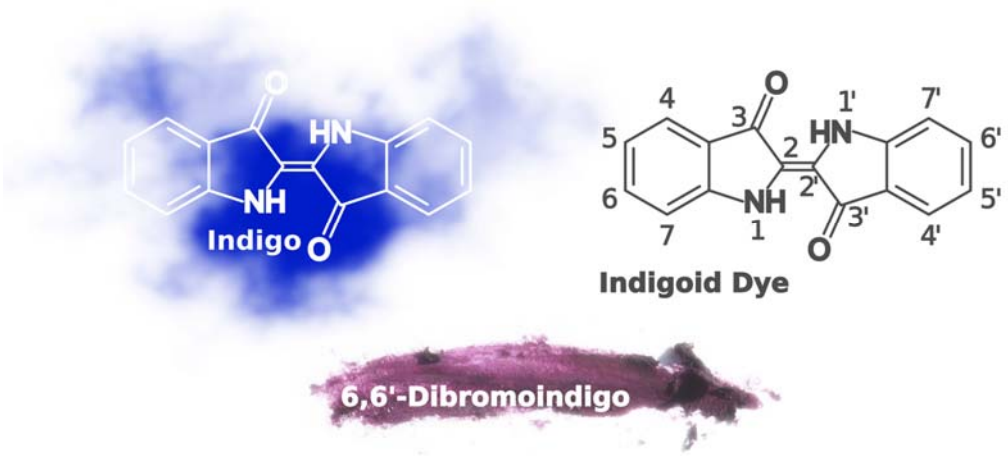

Figure 1 (Left) Structure of the dye indigo shaded with the respective color. (Right) Indigoid dyes are derivatives of indigo that can differ in color and chemical properties. (Middle) The most prominent representative is Tyrian purple, which owns two bromide substituents at position 6 and 6'. The figure shows this valuable dye produced in this study smoothed over a sheet of paper.

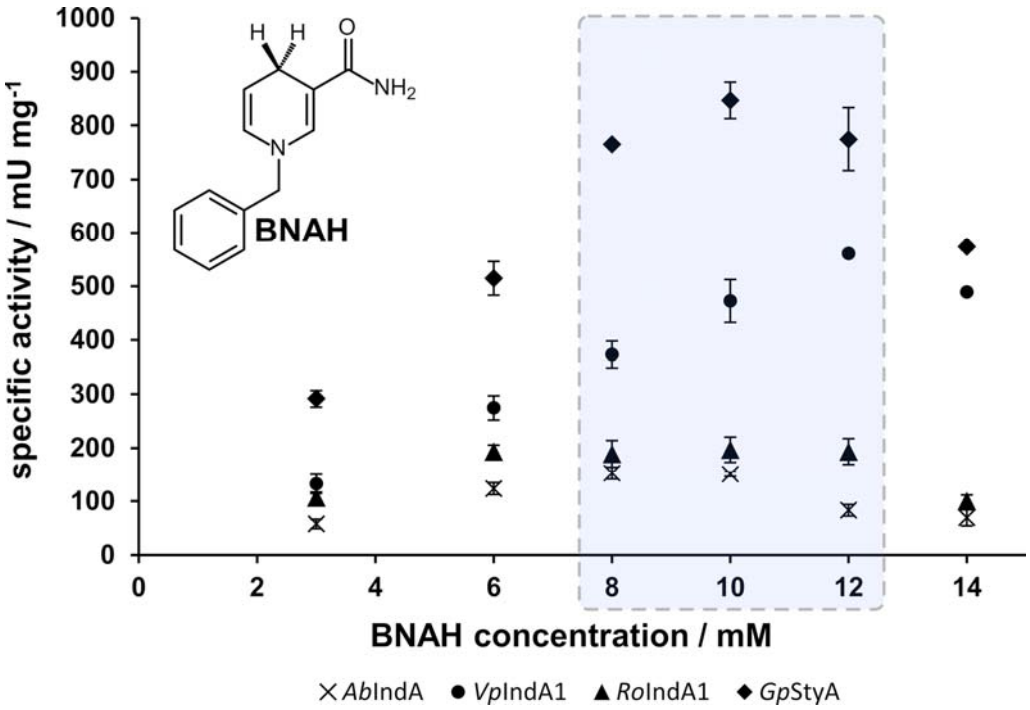

Figure 2 Optimization of BNAH concentration for the monooxygenase assay and biotransformation. The reaction was followed the standard assay with varying concentrations of the electron donor 1-benzyl-1,4-dihydronicotinamide (BNAH). The optimal BNAH

concentration for the monooxygenases is located between 8 and 12 mM (blue box). The chemical structure of BNAH is indicated.

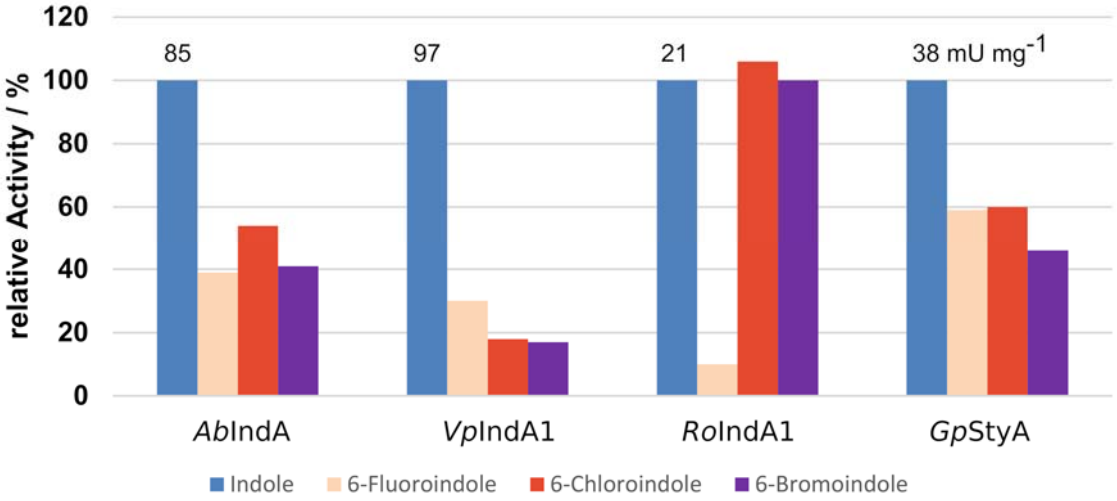

Figure 3 Several halogenated indole derivatives were applied as substrates for GEMs. The shown relative activities refer to the determined activity with indole, which is indicated above the respective bars.

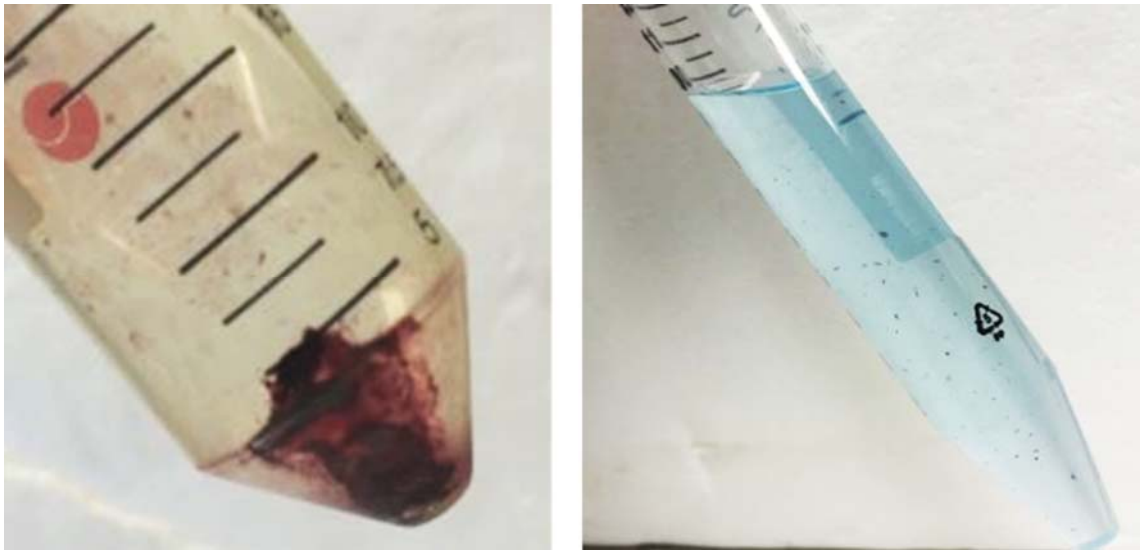

Figure 4 The product of 6-Bromoindole conversion by *Gp*StyA: Tyrian purple. About 5 mg of Tyrian purple were obtained from biotransformation, extraction and vacuum drying (left) and it was dissolved to a great extent in dimethyl sulfoxide (right) prior spectral analysis.

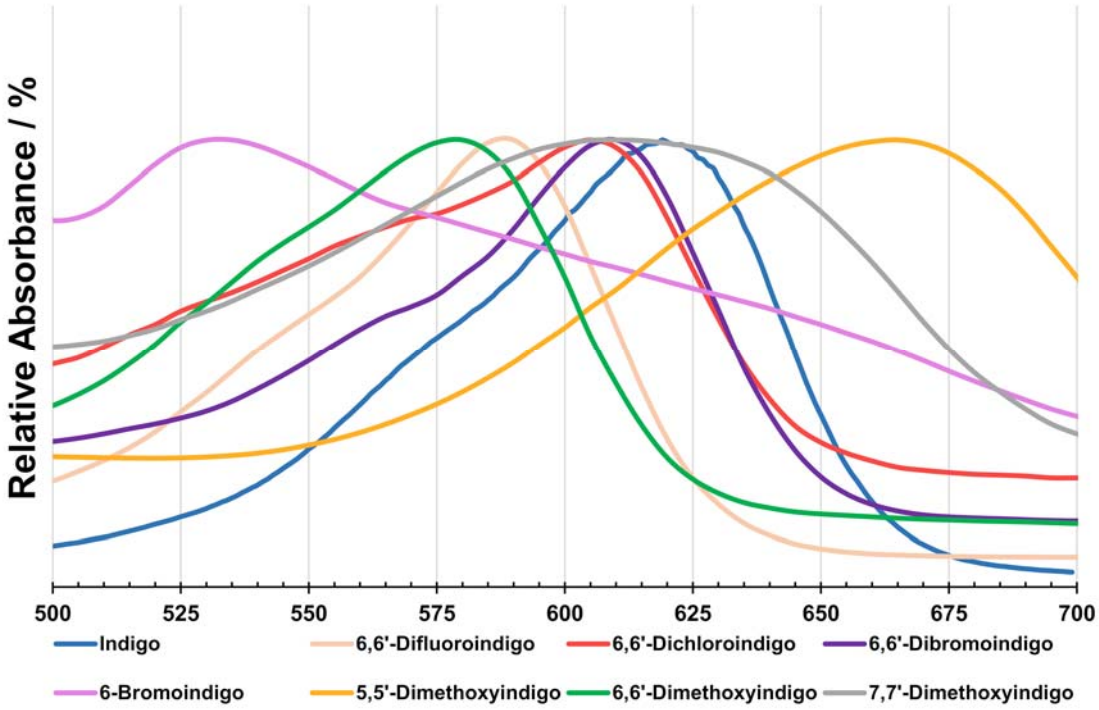

Figure 5 UV/Vis-spectral analysis of the indigoid dyes dissolved in DMSO. The purified indigoid pigments were employed for the determination of extinction coefficients (Table 1).

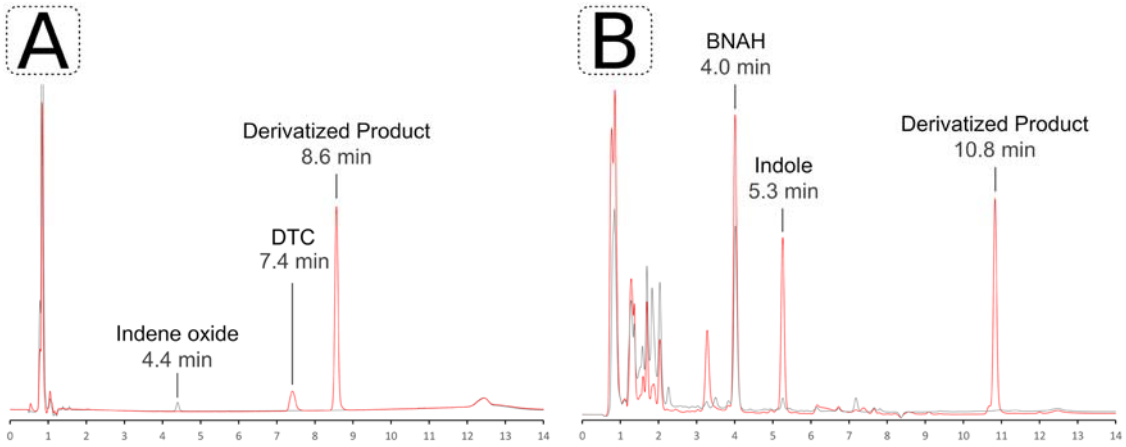

Figure 6 RP-HPLC chromatograms showing DTC derivatization of (A) the control indene oxide and (B) an *Ab*IndA conversion of indole. Reference assays without DTC are shaded in grey while derivatization assays with DTC are shaded in red.

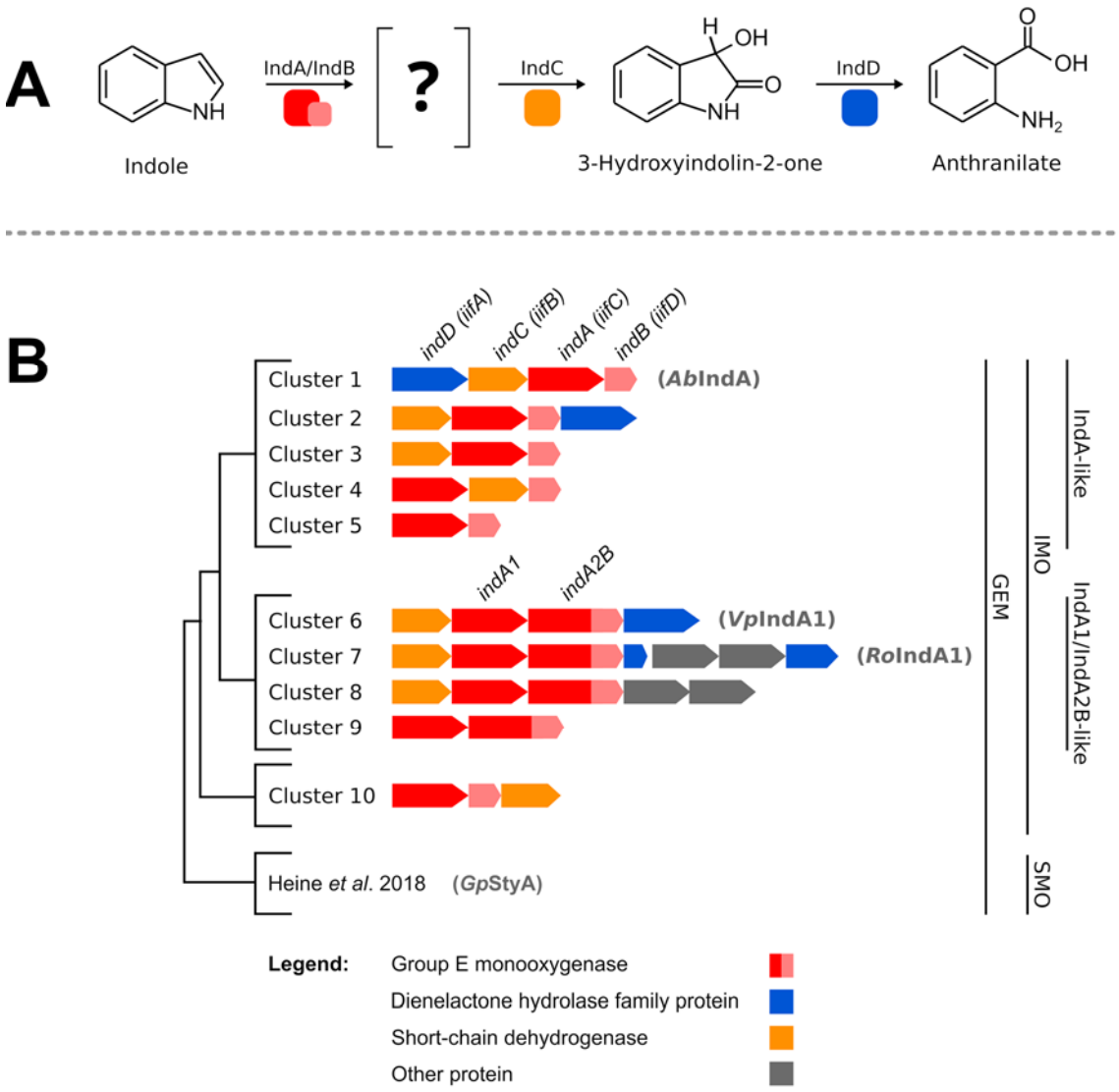

Figure 7 (A) Proposed degradation pathway for indole. The product of the monooxygenase is so far nor known. However, should be transformed by the activity of IndC to 3-Hydroxyindolin-2-one and by IndD to the central intermediate anthranilate (Sadauskas *et al.*, 2017).

(B) Comparison of IMO-related gene clusters. Representative strains for each core gene cluster are listed in Table 2 together with associated aromatic compound degradation genes. The designation of the genes was adapted according to the succession in the indole degradation pathway, where the monooxygenase is the initiating enzyme (see also Qu *et al.*, 2017; Heine *et al.*, 2018 b). Styrene degradation-related gene clusters can be found in Heine *et al.*, (2018c).

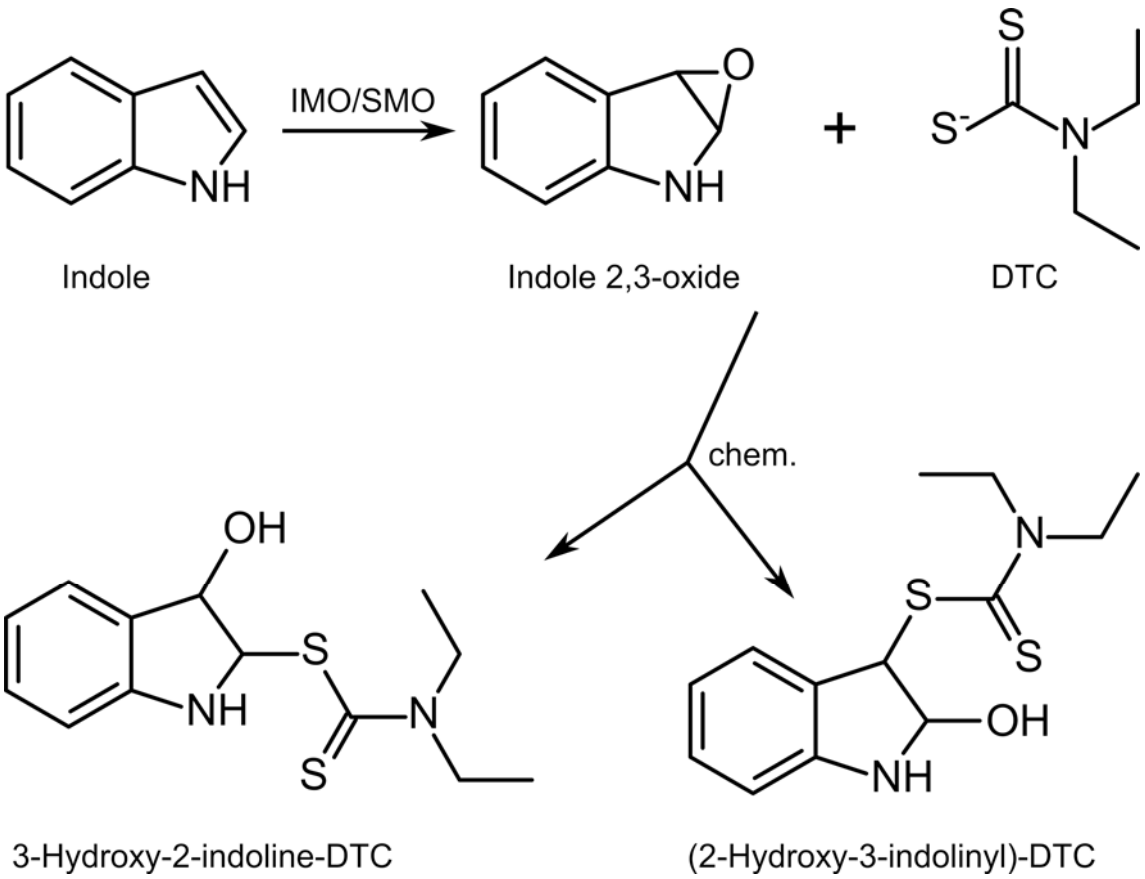

Scheme 1 Illustration of the indole derivatization with DTC following the method of Dupard-Julien *et al.*, (2007). Herein, indole is epoxidized by a GEM to indole 2,3-oxide. This epoxide can now react with DTC to form stable esters that can be separated and identified by mass spectrometry. Unreacted DTC can be decomposed by acidification.

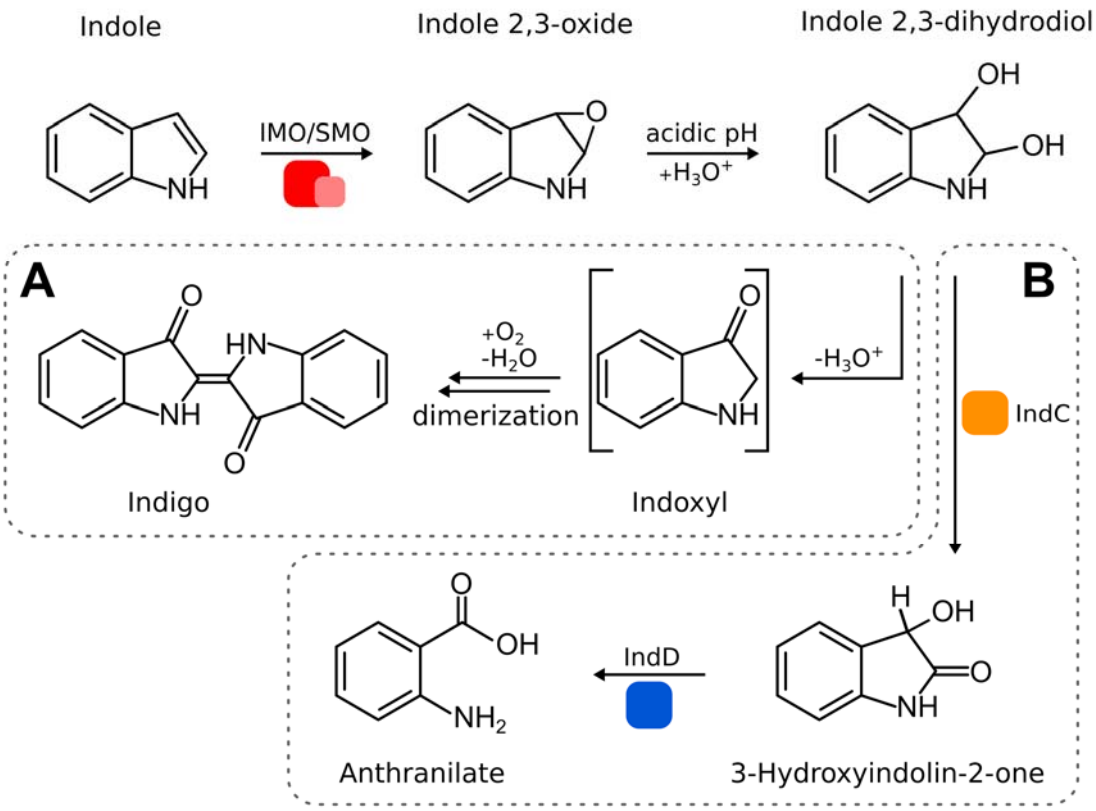

Scheme 2 The predicted reaction mechanism for the formation of indigo by GEMs. Indole is epoxidized to form indole-2,3-oxide which undergoes chemical or enzymatic hydrolysis to yield an indole-2,3-dihydrodiol. This is subsequently dehydrated to yield indoxyl that spontaneously dimerizes to indigo (A). When the enzymes IndC and IndD are present, the diol is further degraded to anthranilic acid via 3-hydroxyindolin-2-one (B) (Sadauskas *et al.*, 2017). The tinting of the enzyme shapes is according to Figure 7.

Supplementary Material

Section 1 Derivatization of epoxides in a imo biotransformation.

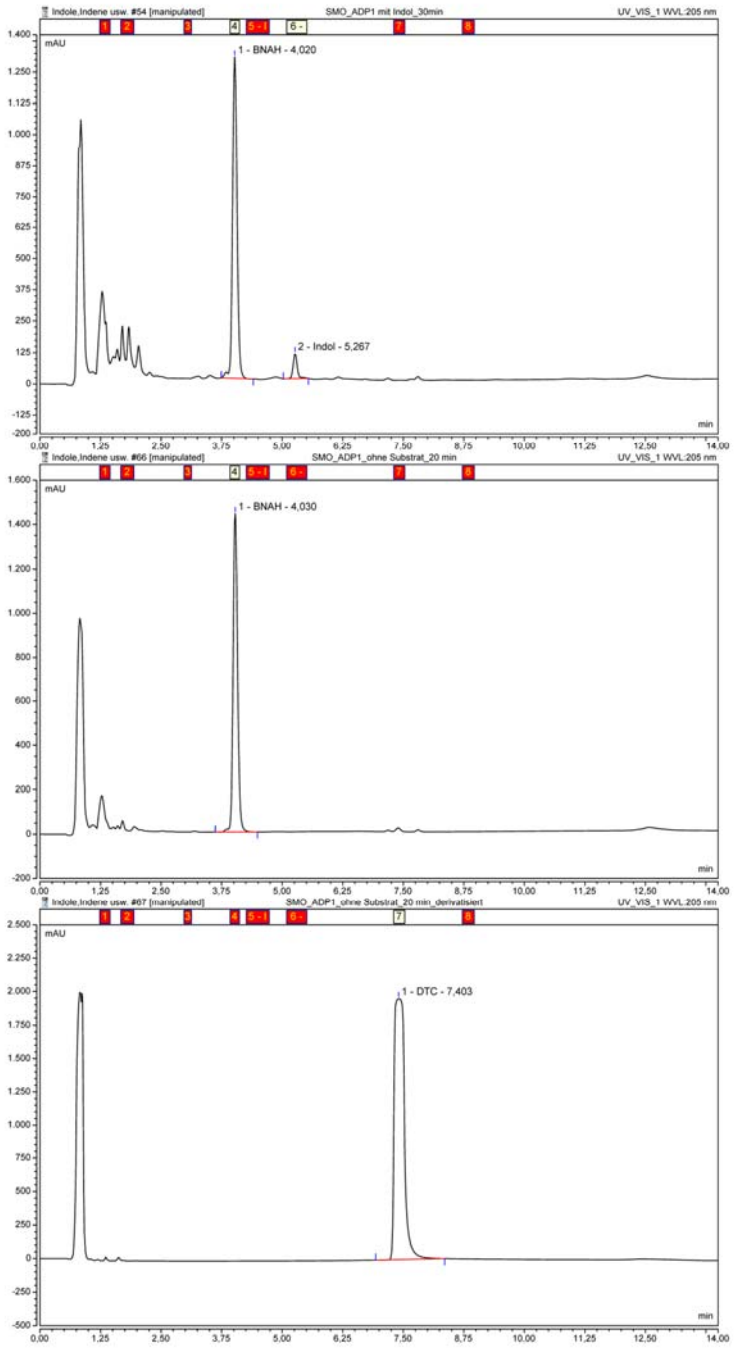

Figure S1 **(Top)** Chromatogram of the reaction products of a 30 min biotransformation of indole by *Ab*IndA without derivatization. The substrate indole elutes after 5.27 min.
(Middle) The nicotinamide cofactor elutes after 4.02 min.
(Bottom) DTC (N,N-diethyldithiocarbamate) elutes after 7.40 min.

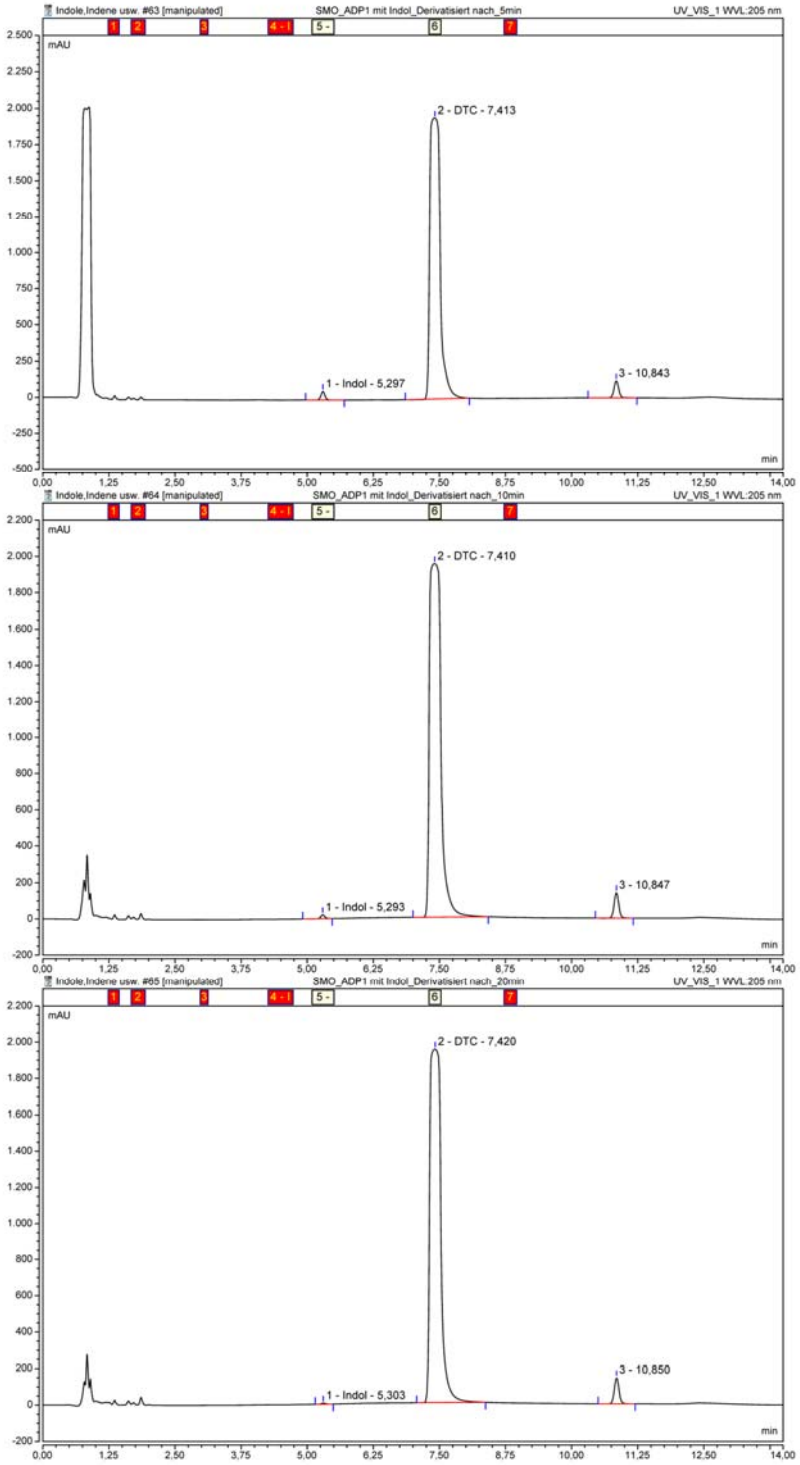

Figure S2 Chromatogram of the reaction products of a 5 to 20 min biotransformation of indole by *Ab*IndA after derivatization with DTC. Herein, DTC derivatization was done after the respective timepoints. The derivatized product elutes after 10.85 min.

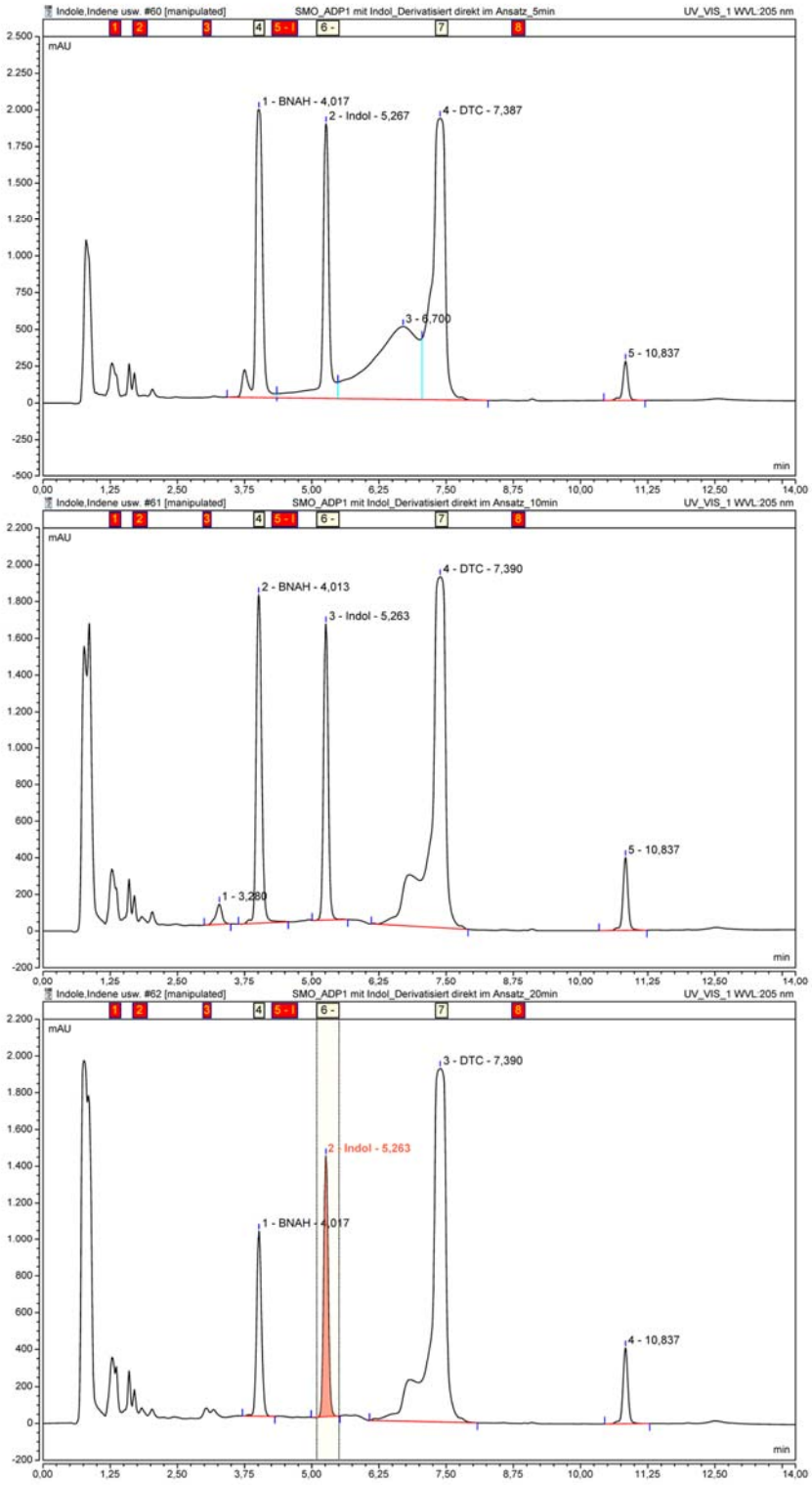

Figure S3 Chromatogram of the reaction products of a 5 to 20 min biotransformation of indole by *Ab*IndA after derivatization with DTC. Herein, DTC was added directly to the reaction mixture to extract the formed epoxide directly after the enzymatic formation. The derivatized product elutes after 10.84 min.

Section 2 HPLC chromatogramms of (derivatized) controls

1. Indol

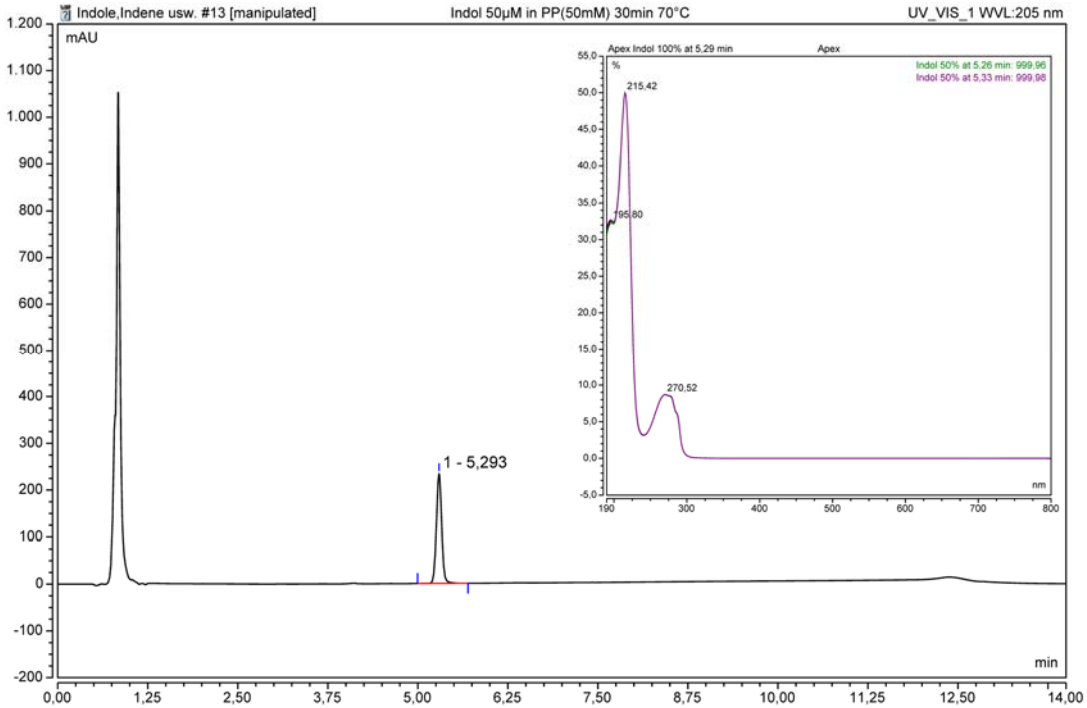

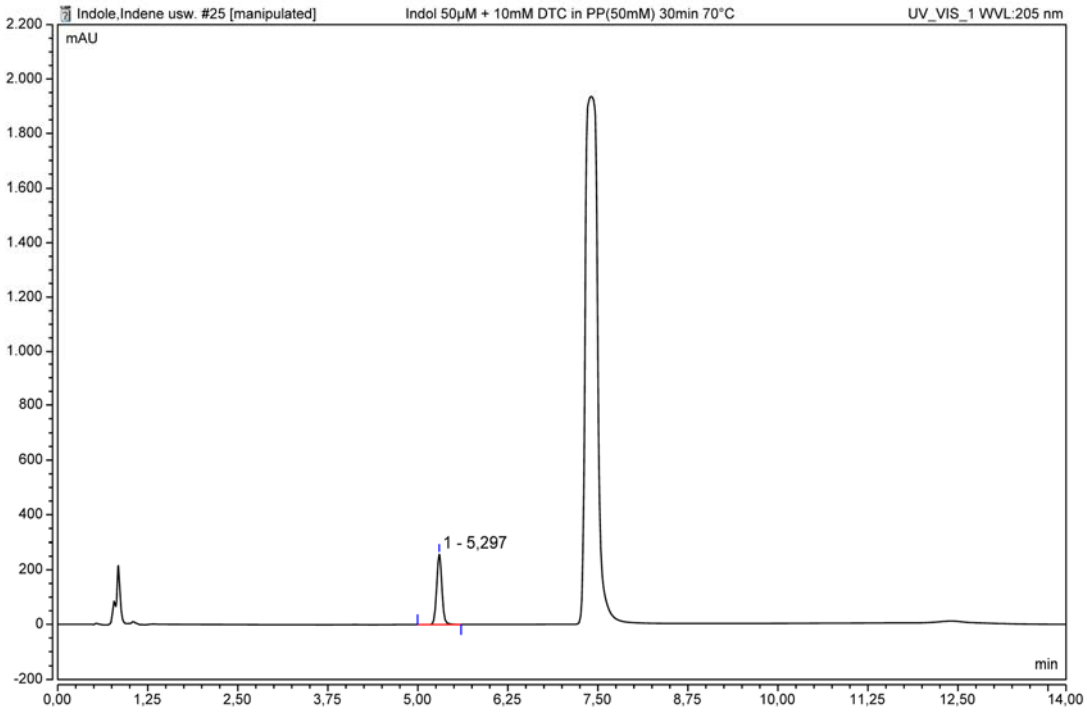

2. 1-Indanol

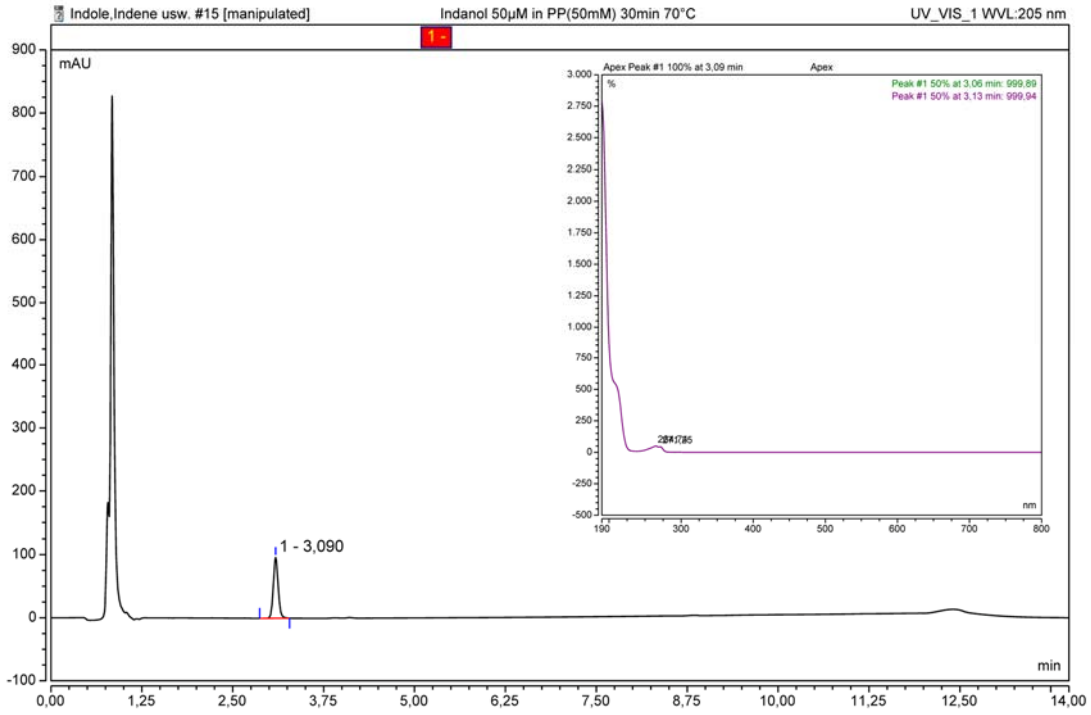

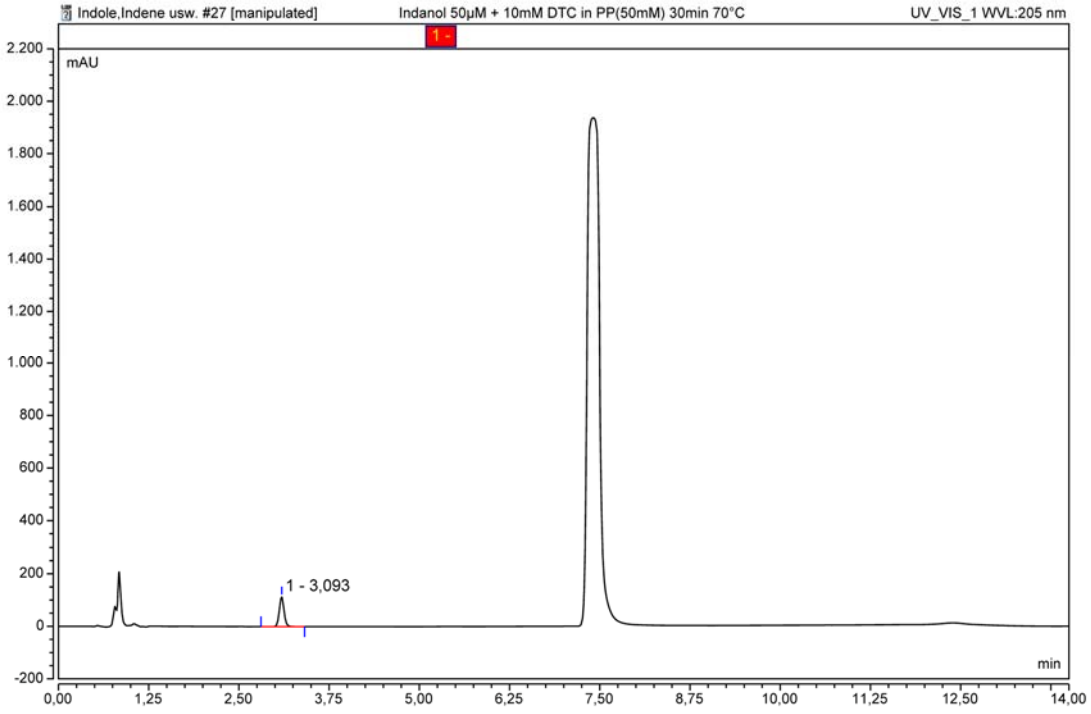

3. Indeneoxid

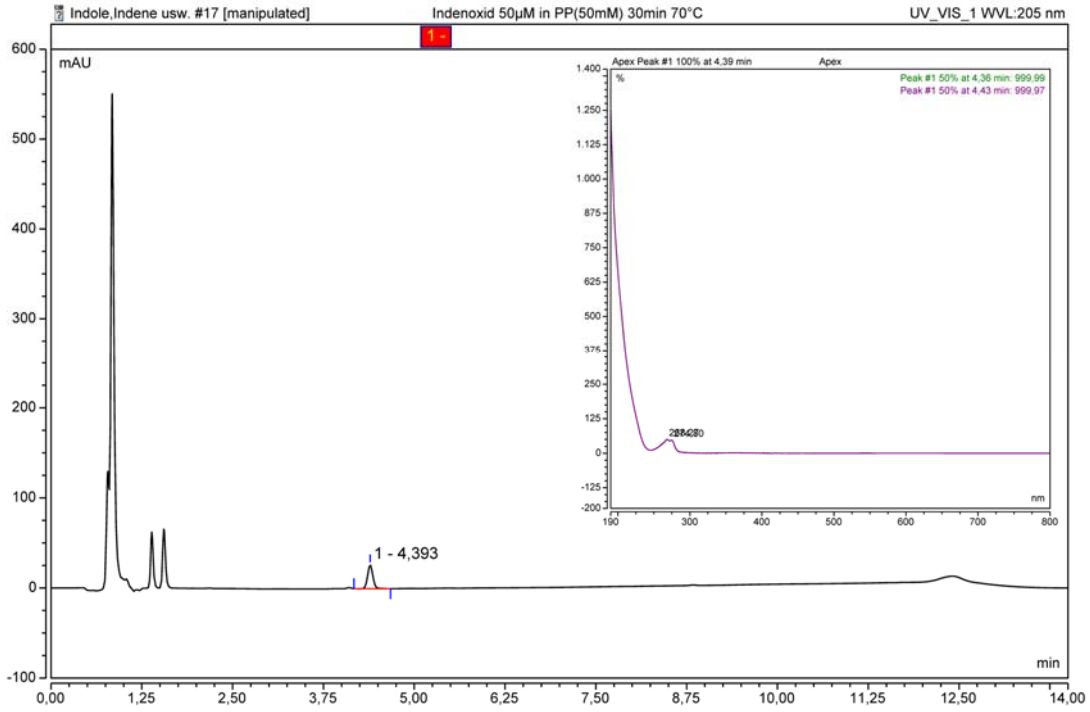

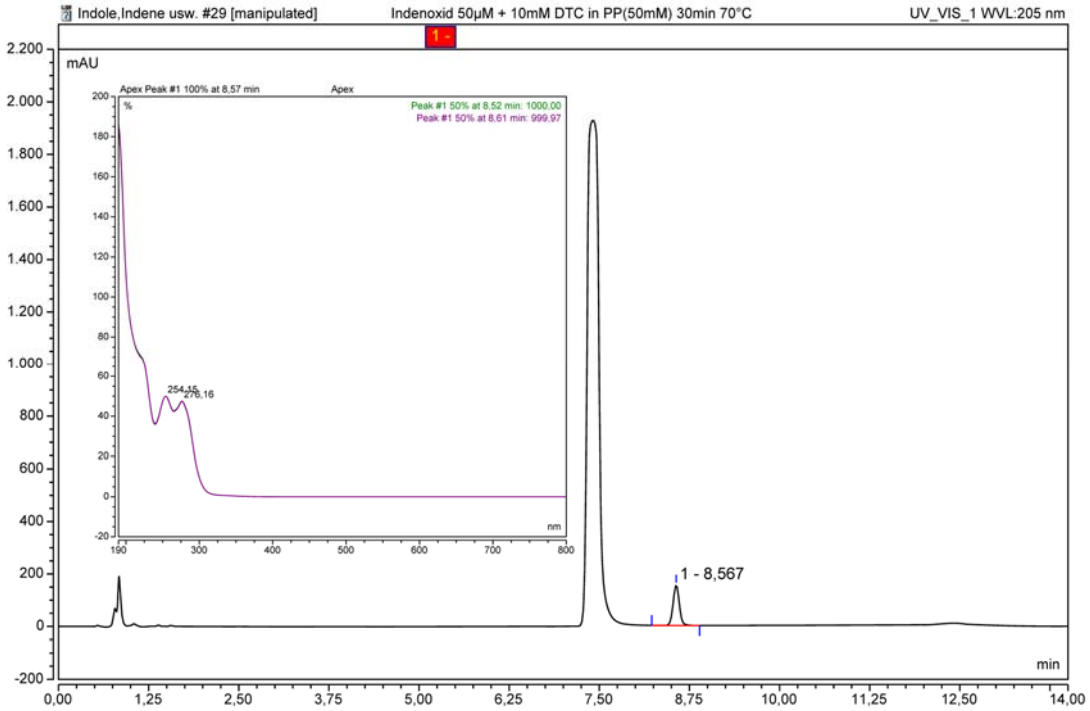

4. Isatin

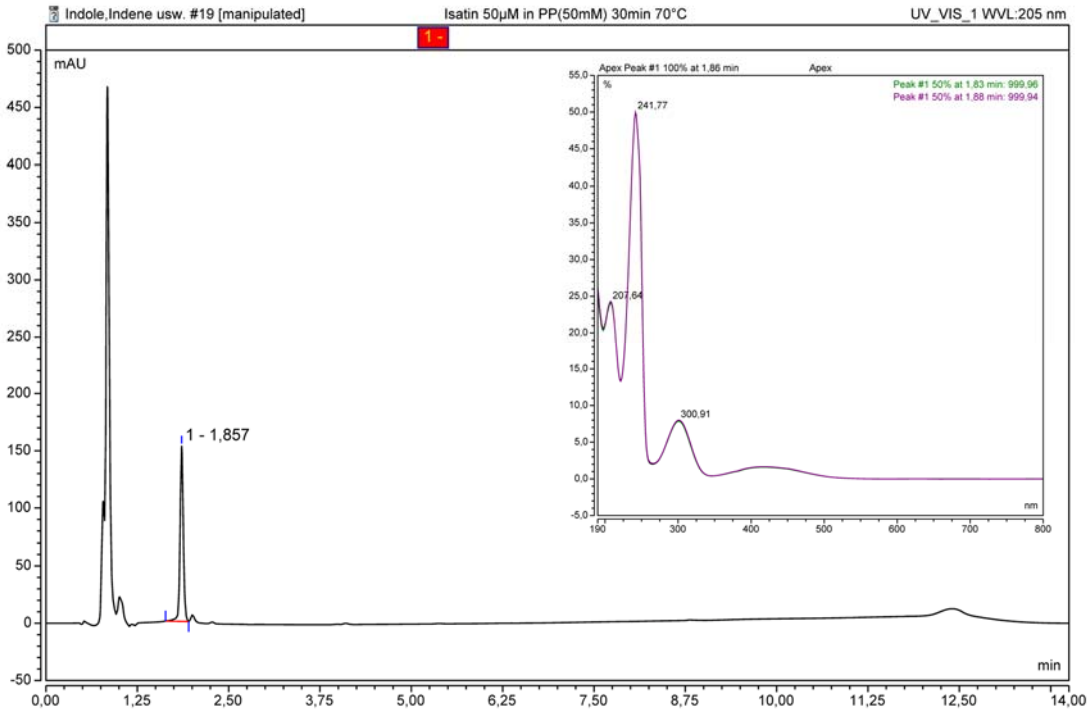

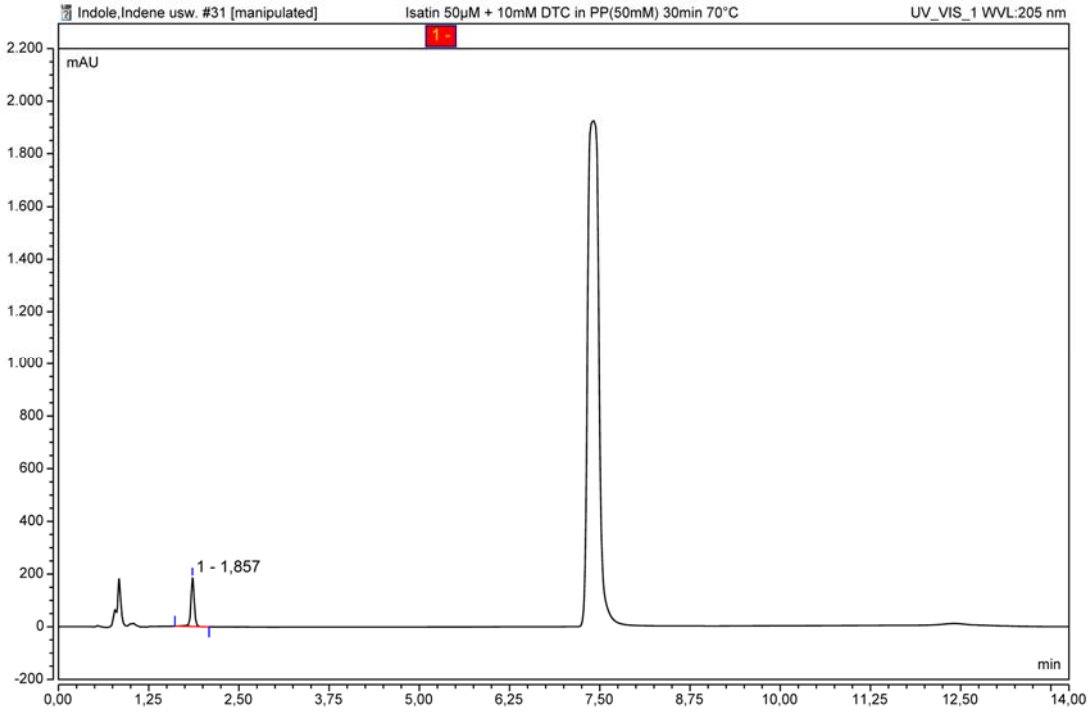

5. Phenylethandiol

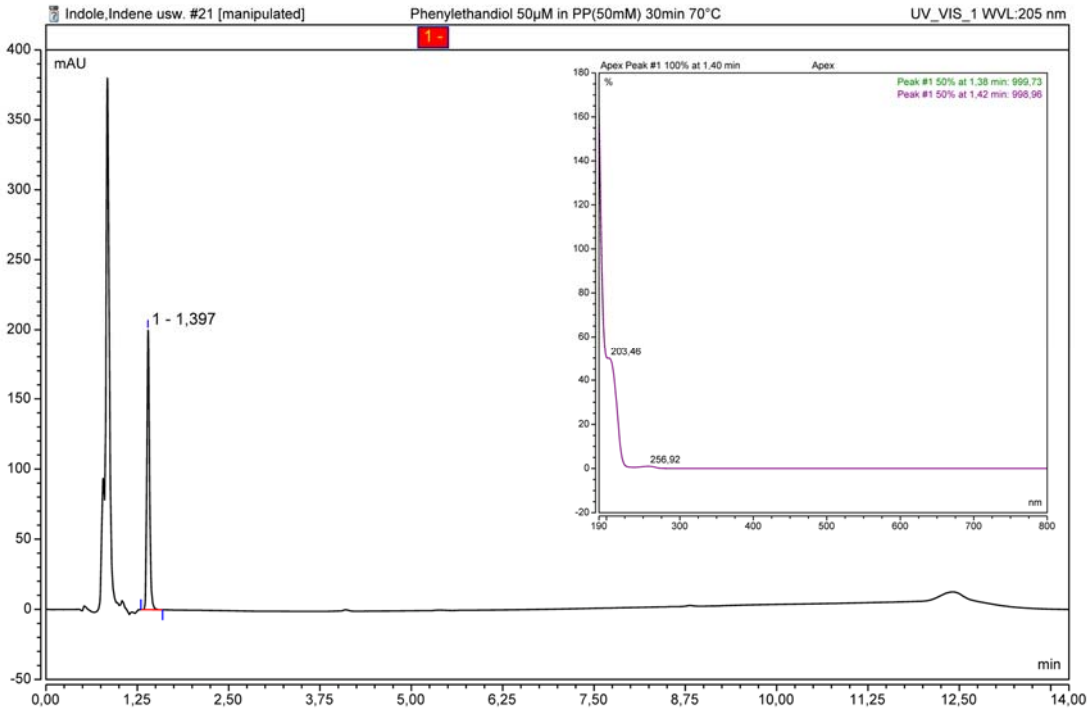

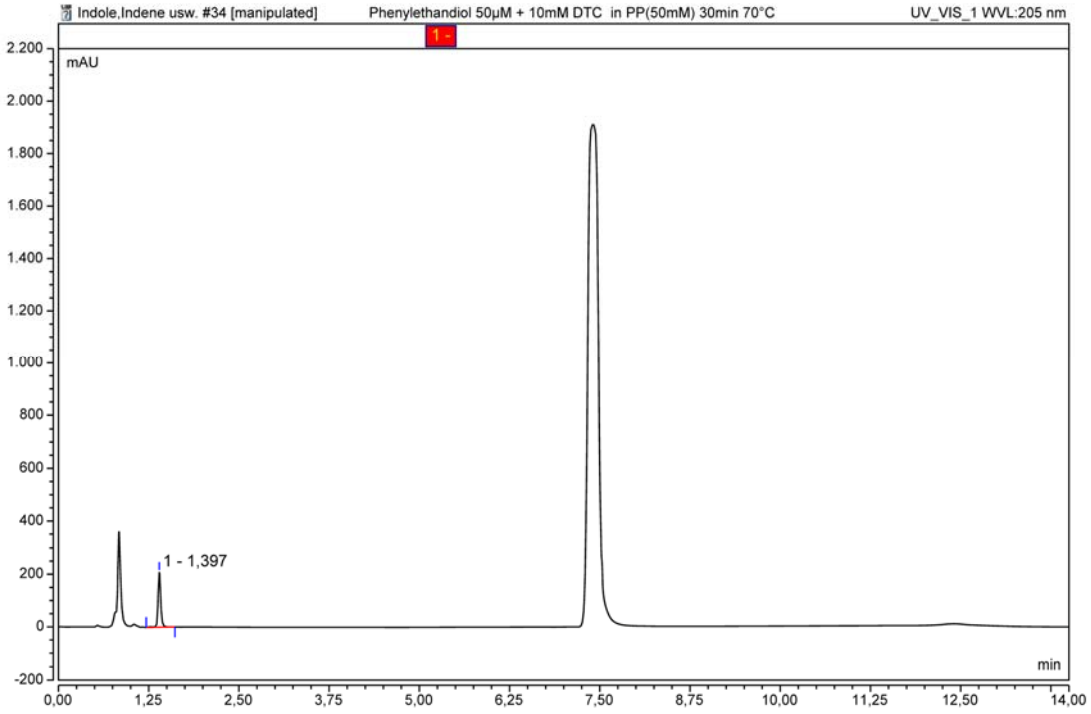

6. Inden

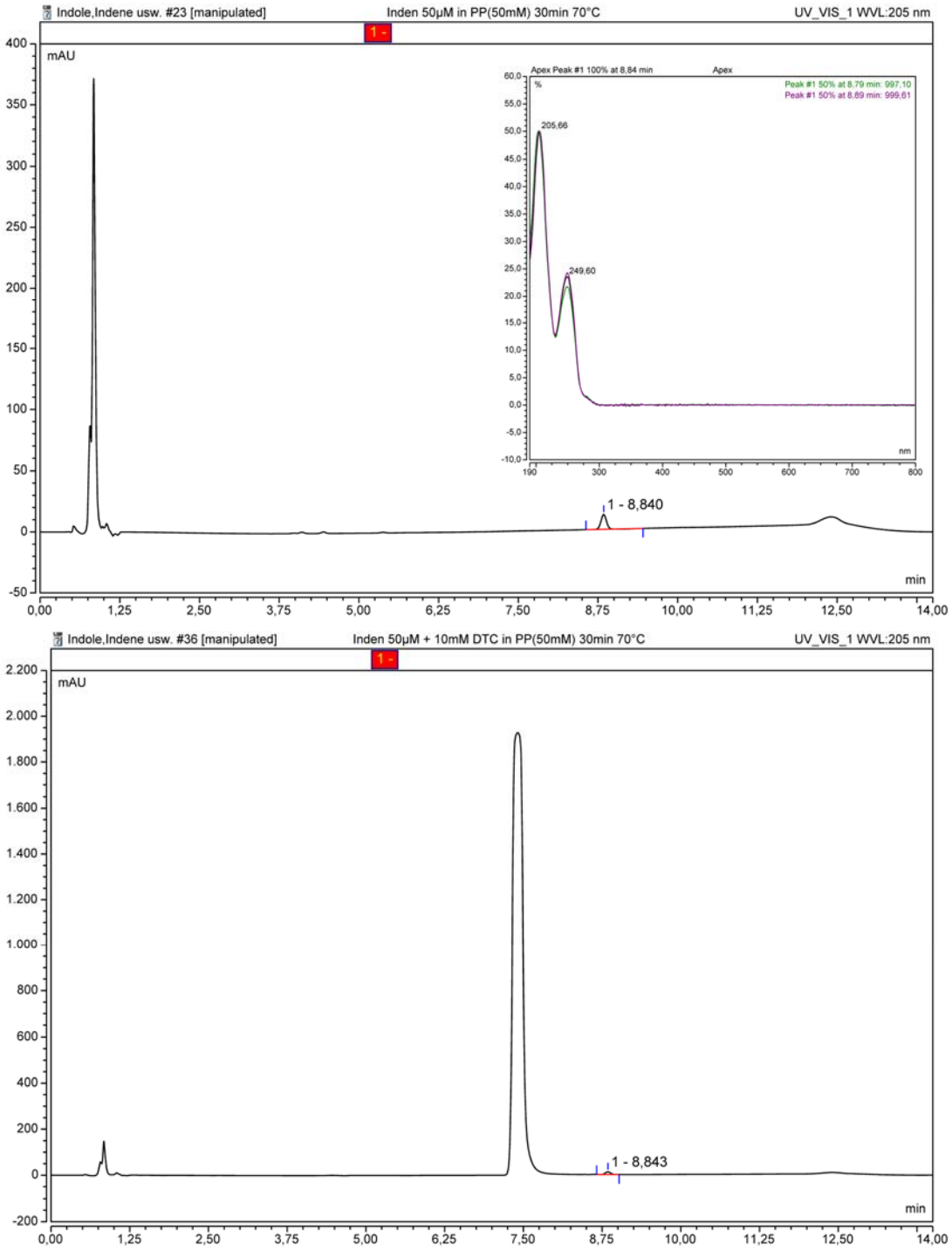

7. RP-HPLC profile and spectra of reference compounds without treatment

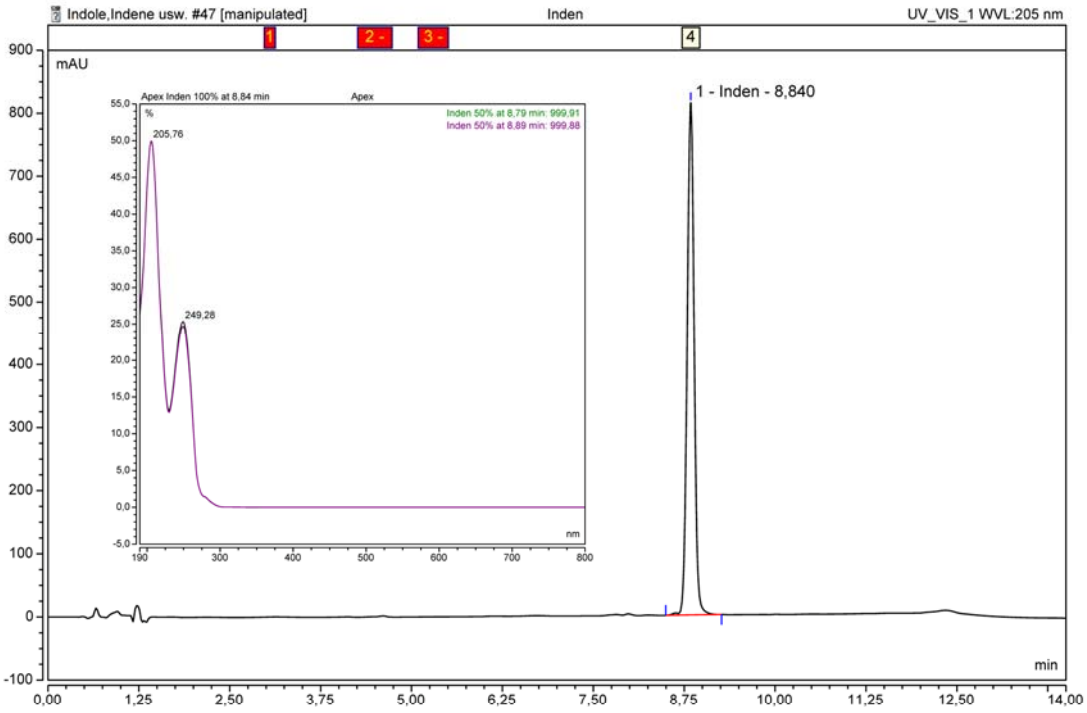

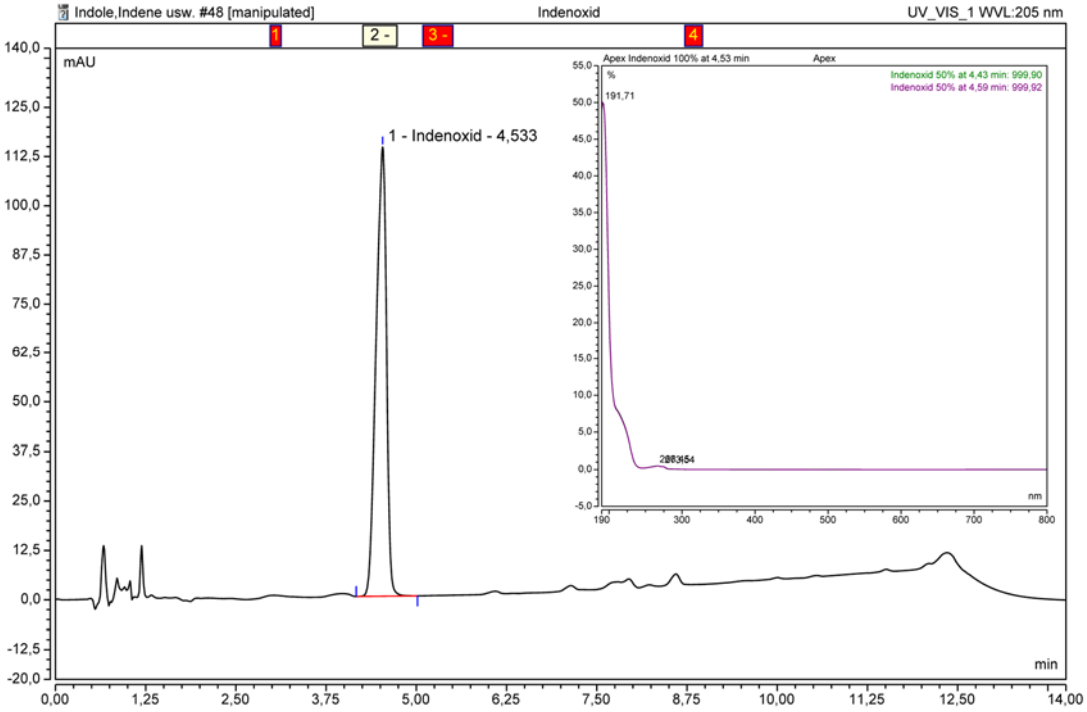

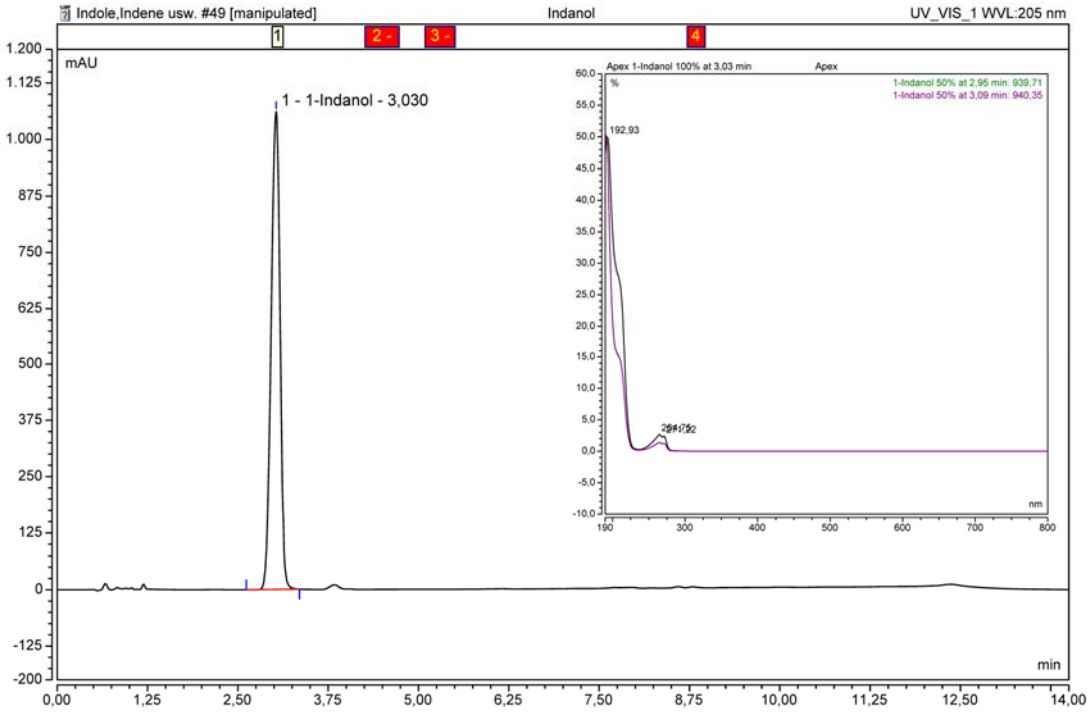

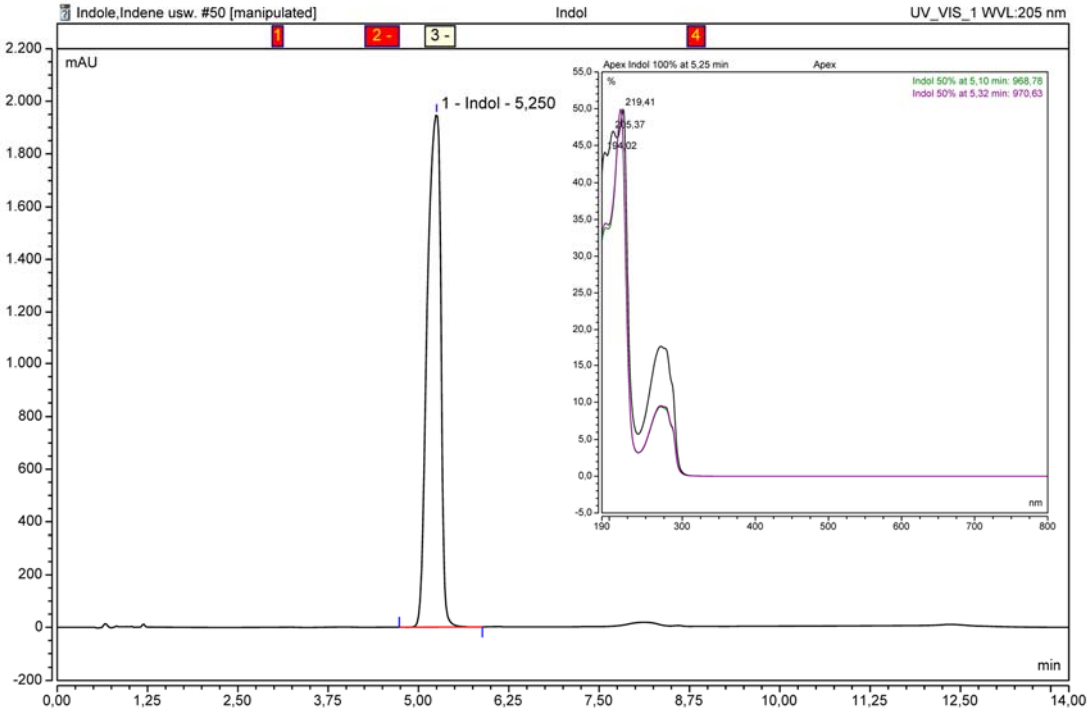

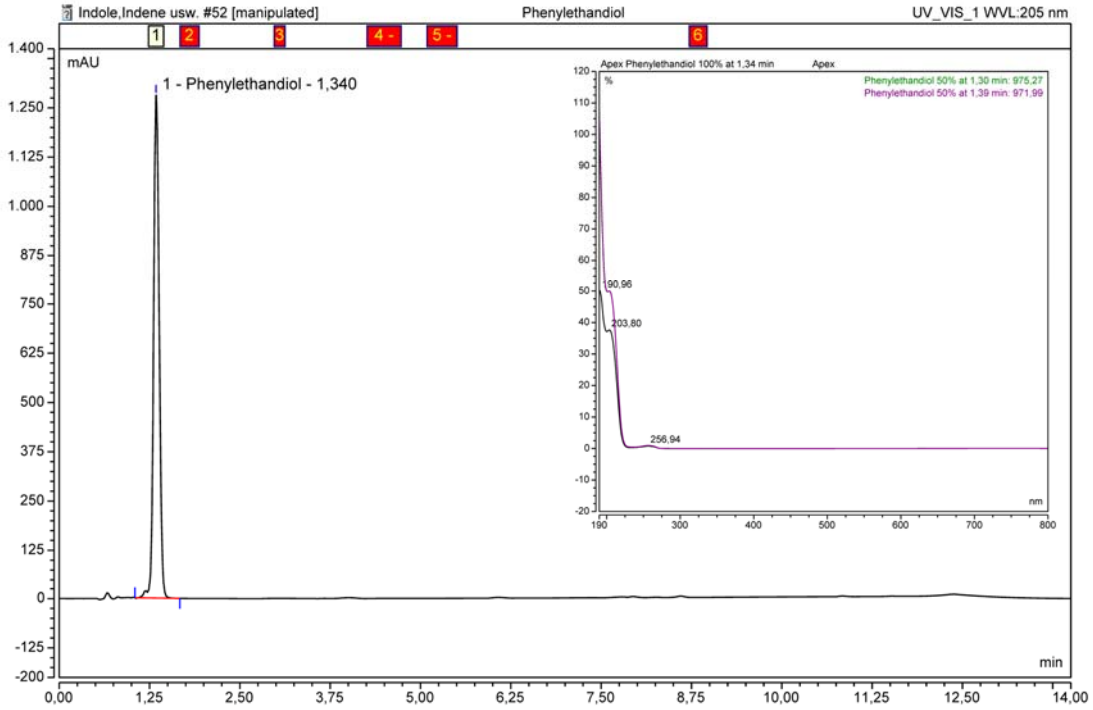

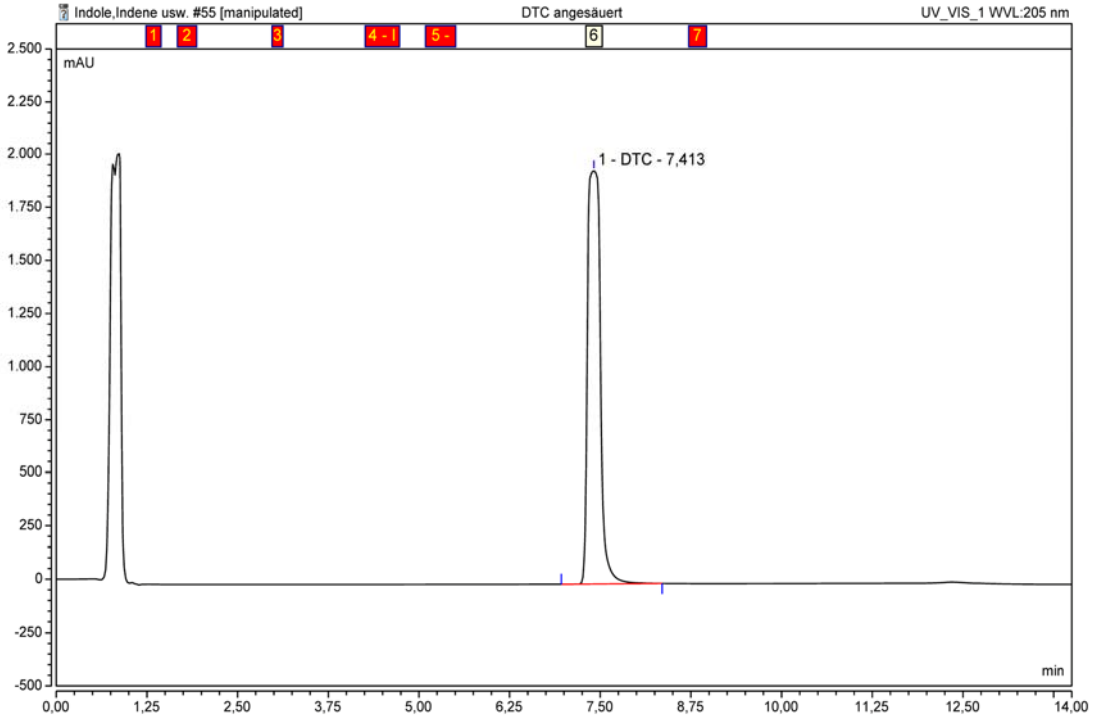

Table S1. FT-ICR-MS assignment of the DTC ester from indole oxide derivatization.

Product	Molecular ion	Observed m/z	Calculated m/z	Sum formula
Derivatized Product	$[M-H]^-$	281.078783	281.078779	$C_{13}H_{17}N_2OS_2$

Section 3 FT-ICR-MS Spectra Of Indigoid Dyes

The measured spectra are shaded in red compared to the calculated spectra in green.

1. 5,5'-Dimethoxyindigo $M^{-\bullet}$

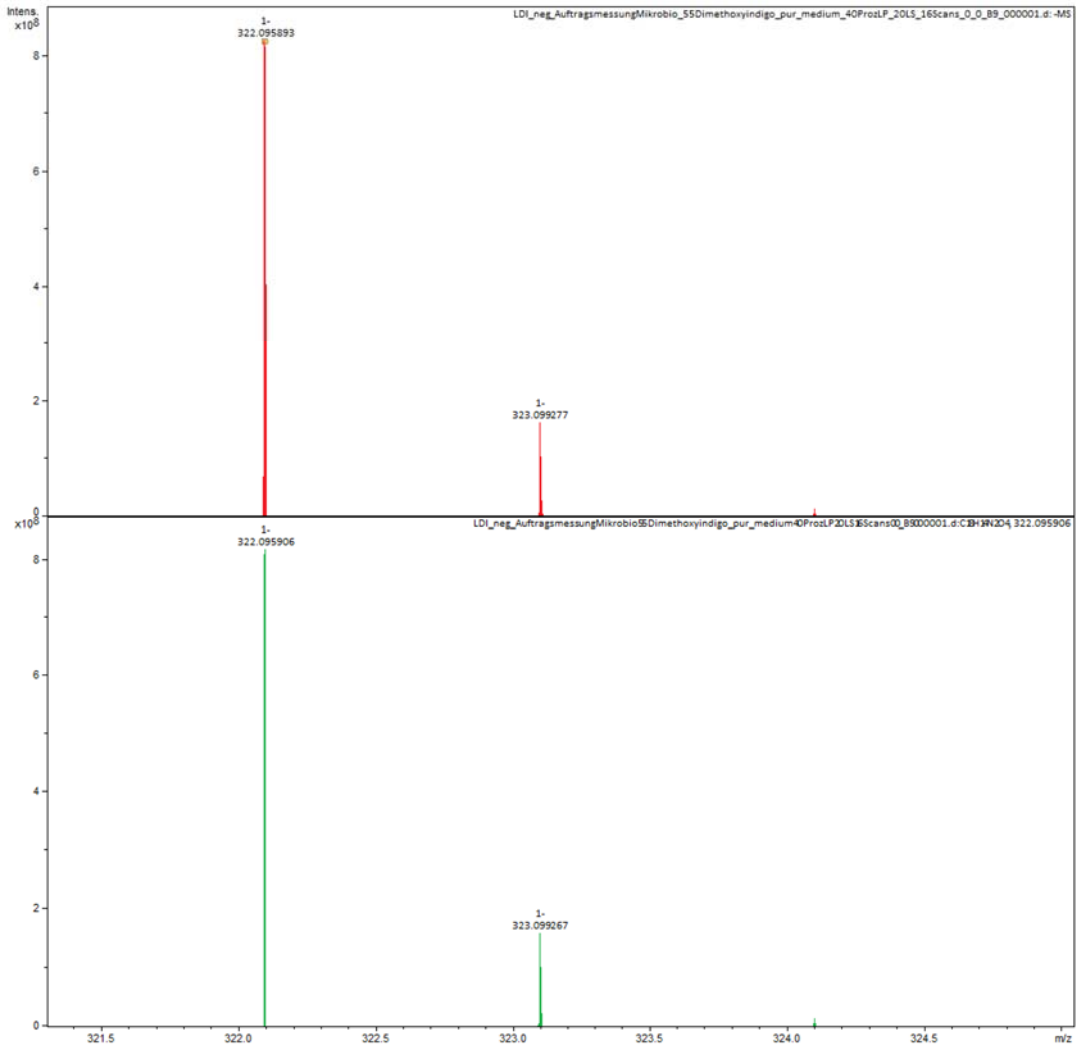

2. 6,6'-Dimethoxyindigo $M^{-\bullet}$

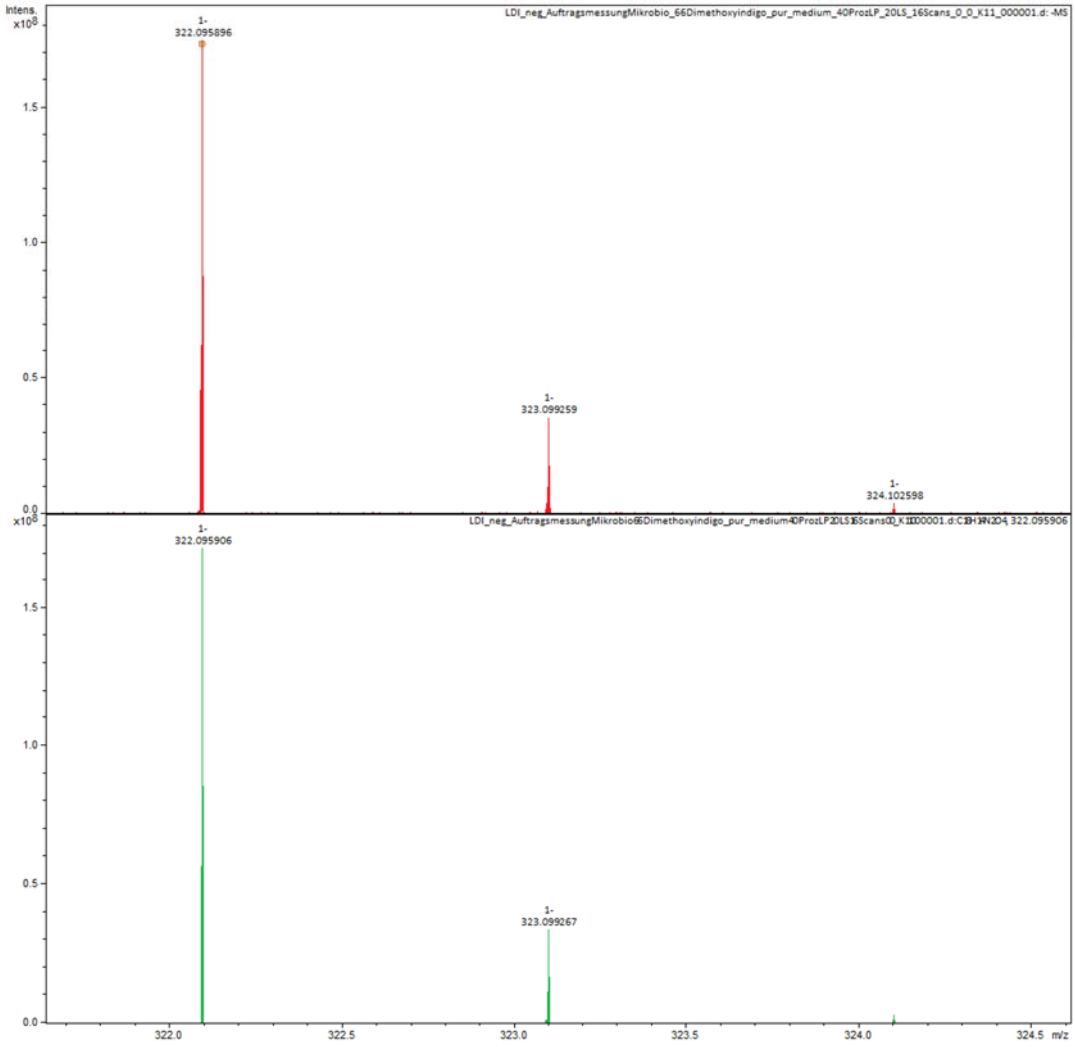

3. 7,7'-Dimethoxyindigo $M^{-\bullet}$

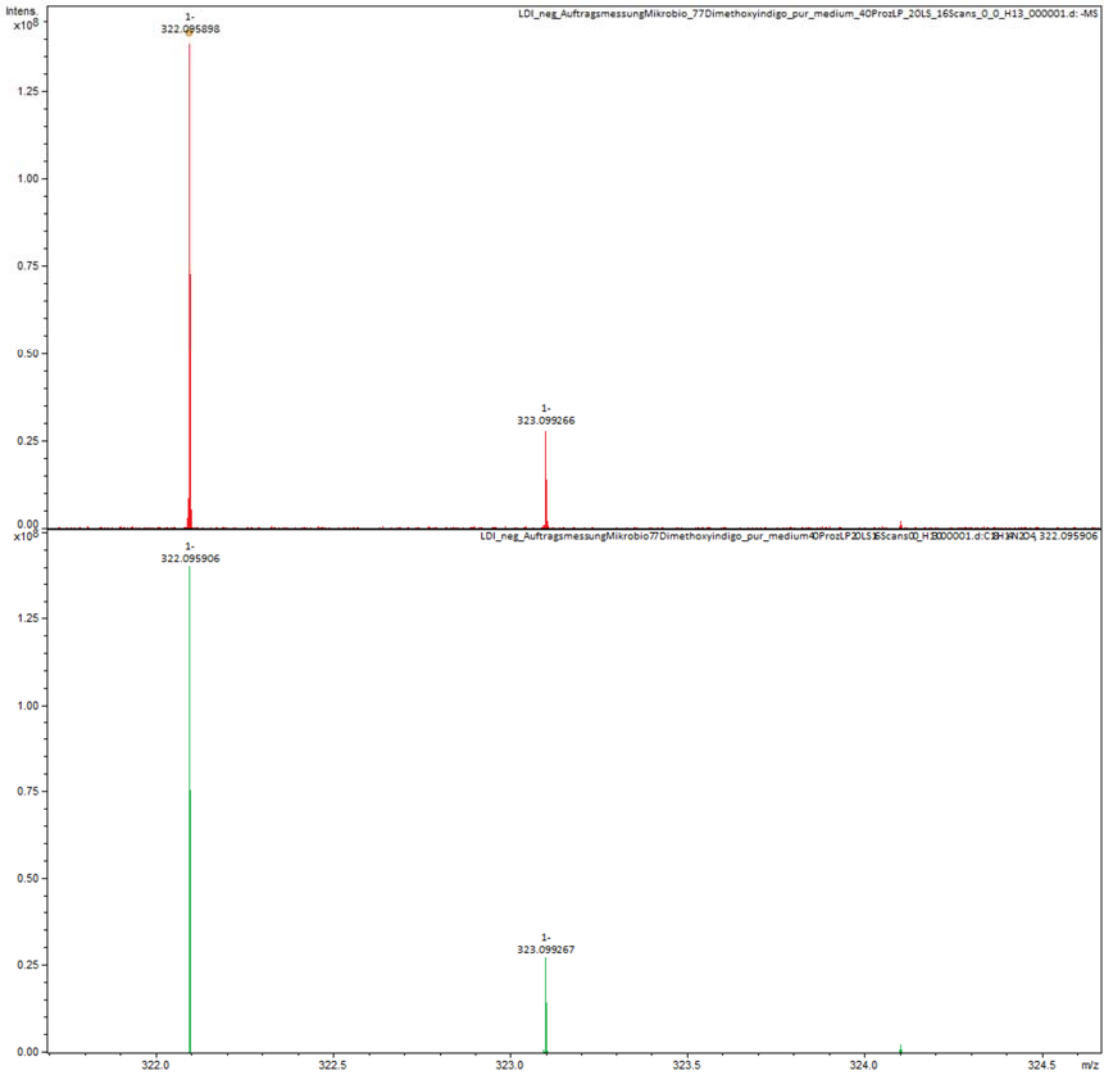

4. 6,6'-Difluoroindigo $M^{-\bullet}$

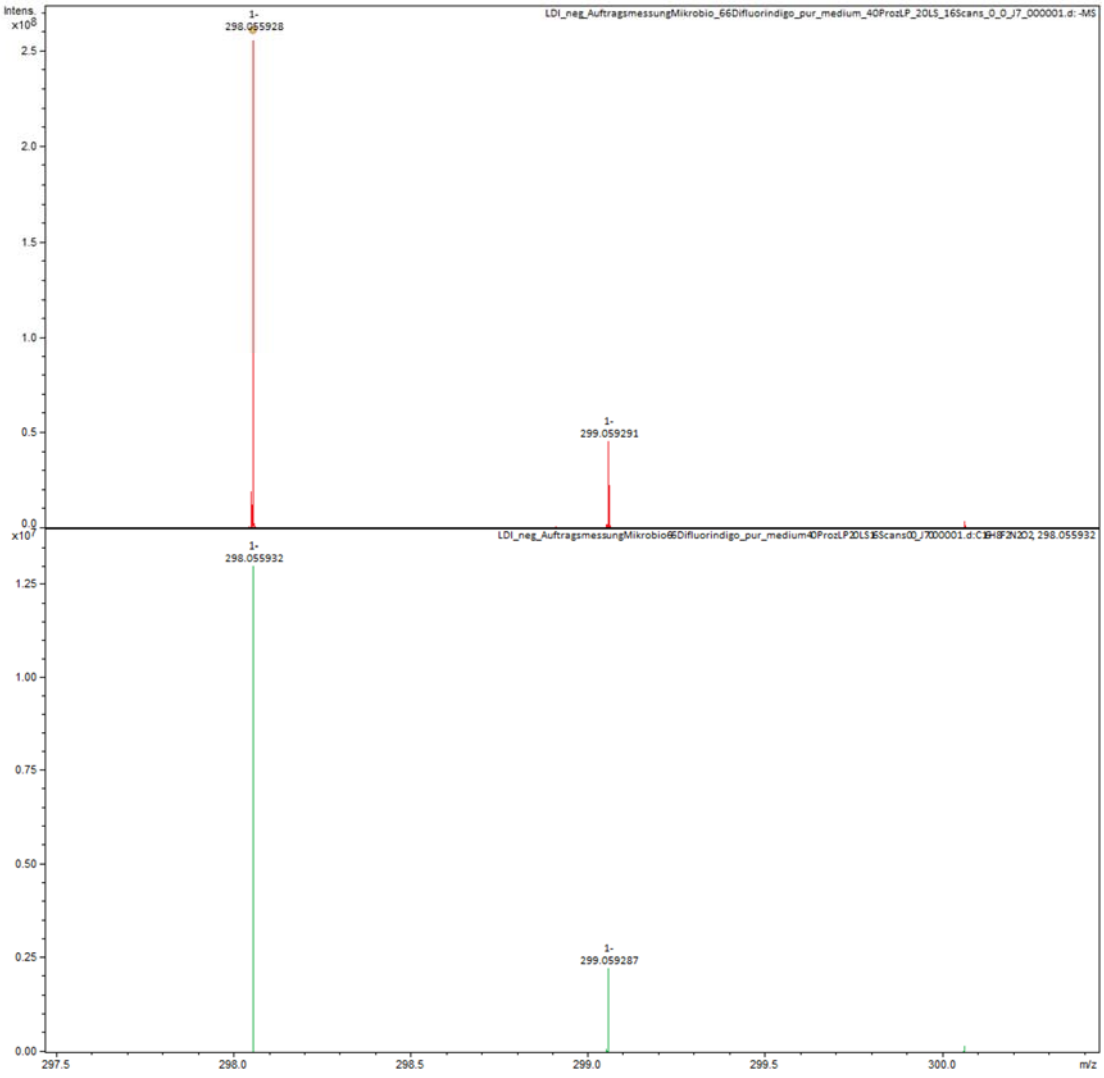

5. 6,6'-Dichloroindigo $M^{-\bullet}$

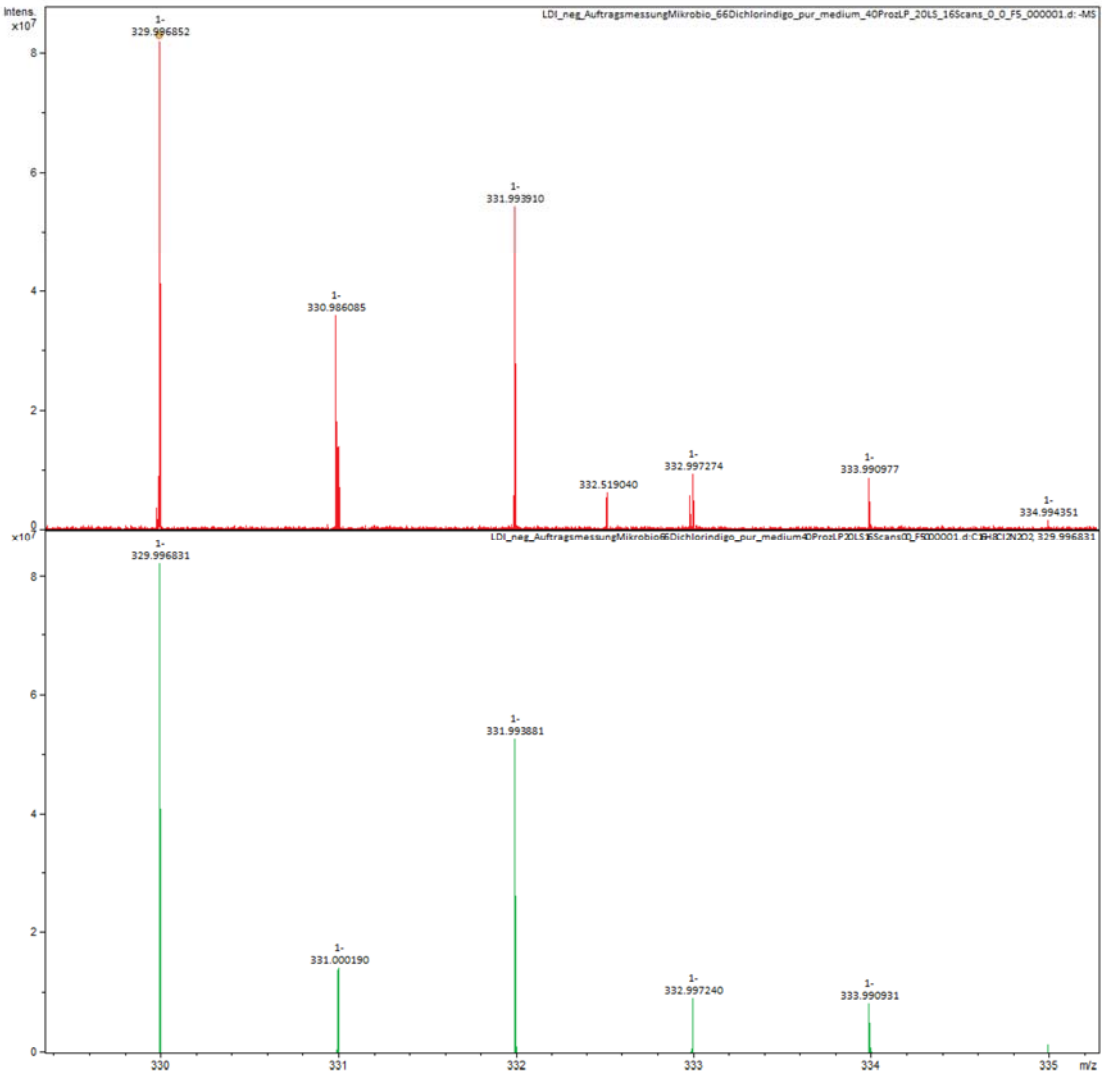

6. 6,6'-Dibromoindigo $M^{-\bullet}$

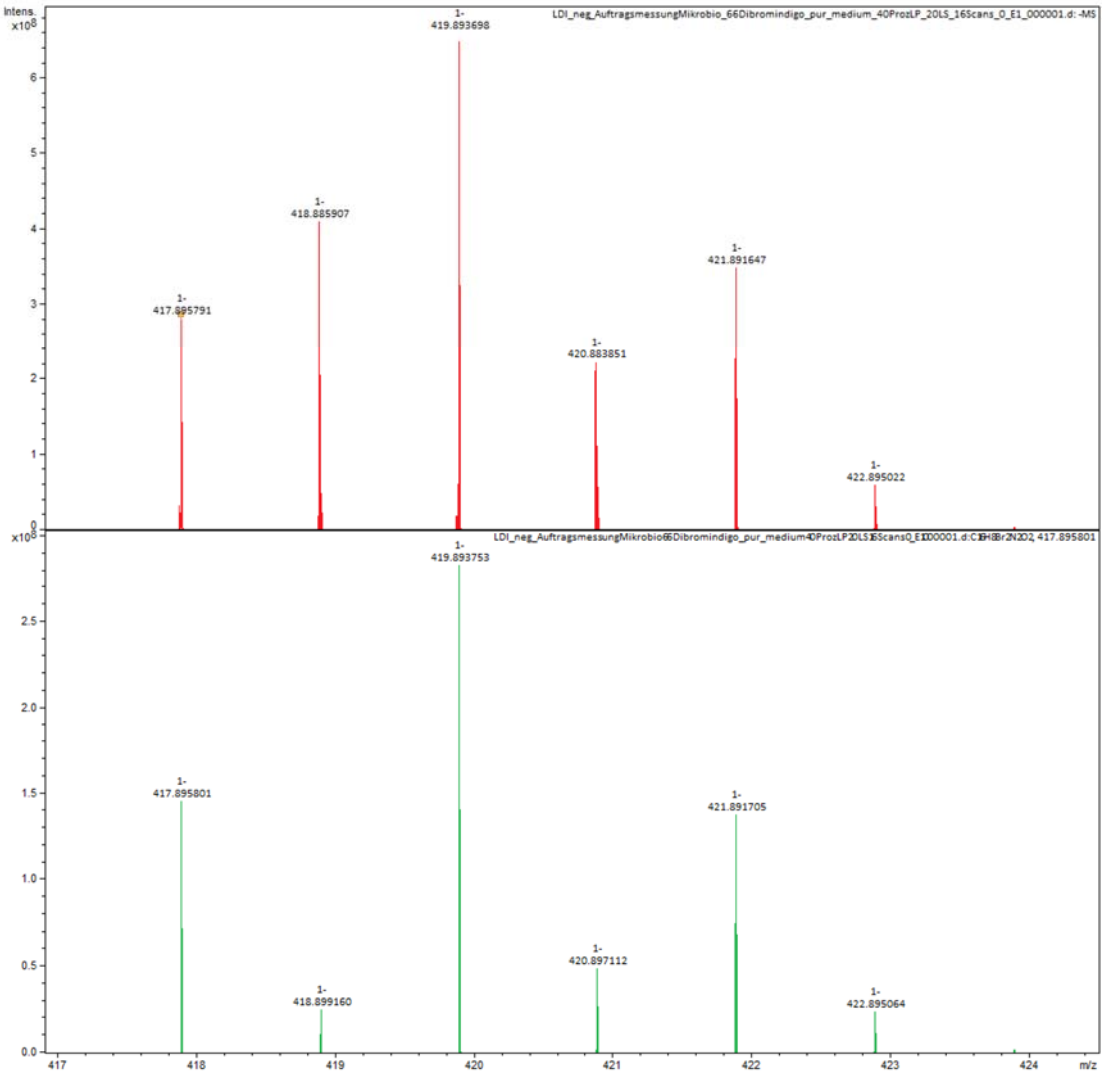

Table S2. FT-ICR-MS assignment of indigoid dyes.

Product	Molecular ion	Observed m/z	Calculated m/z	Sum formula
6,6'-Difluoroindigo	$M^{-\bullet}$	297.048114	297.048107	$C_{16}H_7F_2N_2O_2$
	$[M-H]^-$	298.055928	298.055932	$C_{16}H_8F_2N_2O_2$
6,6'-Dichloroindigo	$M^{-\bullet}$	328.989019	328.989006	$C_{16}H_7Cl_2N_2O_2$
	$[M-H]^-$	329.996839	329.996831	$C_{16}H_8Cl_2N_2O_2$
6,6'-Dibromoindigo	$M^{-\bullet}$	416.887970	416.887976	$C_{16}H_7Br_2N_2O_2$
	$[M-H]^-$	417.895791	417.895801	$C_{16}H_8Br_2N_2O_2$
5,5'-Dimethoxyindigo	$M^{-\bullet}$	321.088099	321.088080	$C_{18}H_{13}N_2O_4$
	$[M-H]^-$	322.095893	322.095906	$C_{18}H_{14}N_2O_4$
6,6'-Dimethoxyindigo	$M^{-\bullet}$	321.088087	321.088080	$C_{18}H_{13}N_2O_4$
	$[M-H]^-$	322.095896	322.095906	$C_{18}H_{14}N_2O_4$
7,7'-Dimethoxyindigo	$M^{-\bullet}$	321.088090	321.088080	$C_{18}H_{13}N_2O_4$
	$[M-H]^-$	322.095898	322.095906	$C_{18}H_{14}N_2O_4$